Interaction of a Cumulus Cloud Ensemble with the Large-Scale Environment, Part I

AKIO ARAKAWA AND WAYNE HOWARD SCHUBERT[1]

Dept. of Meteorology, University of California, Los Angeles 90024

(Manuscript received 10 August 1973, in revised form 7 November 1973)

ABSTRACT

A theory of the interaction of a cumulus cloud ensemble with the large-scale environment is developed. In this theory, the large-scale environment is divided into the subcloud mixed layer and the region above. The time changes of the environment are governed by the heat and moisture budget equations for the subcloud mixed layer and for the region above, and by a prognostic equation for the depth of the mixed layer. In the environment above the mixed layer, the cumulus convection affects the temperature and moisture fields through cumulus-induced subsidence and detrainment of saturated air containing liquid water which evaporates in the environment. In the subcloud mixed layer, the cumulus convection does not act directly on the temperature and moisture fields, but it affects the depth of the mixed layer through cumulus-induced subsidence. Under these conditions, the problem of parameterization of cumulus convection reduces to the determination of the vertical distributions of the total vertical mass flux by the ensemble, the total detrainment of mass from the ensemble, and the thermodynamical properties of the detraining air.

The cumulus ensemble is spectrally divided into sub-ensembles according to the fractional entrainment rate, given by the ratio of the entrainment per unit height to the vertical mass flux in the cloud. For these sub-ensembles, the budget equations for mass, moist static energy, and total water content are obtained. The solutions of these equations give the temperature excess, the water vapor excess, and the liquid water content of each sub-ensemble, and further reduce the problem of parameterization to the determination of the mass flux distribution function, which is the sub-ensemble vertical mass flux at the top of the mixed layer.

The cloud work function, which is an integral measure of the buoyancy force in the clouds, is defined for each sub-ensemble; and, under the assumption that it is in quasi-equilibrium, an integral equation for the mass flux distribution function is derived. This equation describes how a cumulus ensemble is forced by large-scale advection, radiation, and surface turbulent fluxes, and it provides a closed parameterization of cumulus convection for use in prognostic models of large-scale atmospheric motion.

1. Introduction

The many individual cumulus clouds which occur in a large-scale atmospheric disturbance have time and space scales much smaller than the disturbance itself. Because of this scale separation, it may be possible to predict the time change of the large-scale disturbance by describing not each of the many individual clouds, but only their collective influence. This is the goal of cumulus parameterization.

The importance of cumulus convection for large-scale tropical disturbances was recognized through observational studies (Riehl and Malkus, 1958, 1961; Yanai, 1961a, b). The need to parameterize cumulus convection became clear with the failure of early theoretical attempts to explain the size and growth rate of tropical cyclones [see review article by Yanai (1964)]. Recognition of this need led to the classical papers of Charney and Eliassen (1964) and Ooyama (1964), in which the concept of conditional instability of the second kind (CISK) first appeared. In CISK, the cumulus-scale and the cyclone-scale motions cooperate, the cumulus clouds providing the heat which drives the cyclone, and the cyclone providing the moisture which maintains the cumulus clouds. The simple parameterizations used in these papers not only gave insight into this cooperative mechanism, but also led to considerable success in the numerical simulation of tropical cyclones (e.g., Ooyama, 1969).

In spite of this success, these early parameterizations were too crude to be used for more general situations, and several attempts were made to obtain more widely applicable parameterizations [see review articles by Yanai (1971a), Bates (1972) and Ogura (1972)]. These attempts, however, were based on a high degree of empiricism and intuition, and lacked a theoretical framework for describing the mutual interactions between a cumulus ensemble and the large-scale environment.

There is now general agreement on the way in which an existing cumulus cloud ensemble produces time changes in the large-scale temperature and moisture fields (Arakawa, 1969, 1971, 1972; Betts, 1973a, b; Gray, 1972; López, 1972a, b; Ooyama, 1971; Yanai,

[1] Present affiliation: Department of Atmospheric Science, Colorado State University, Fort Collins.

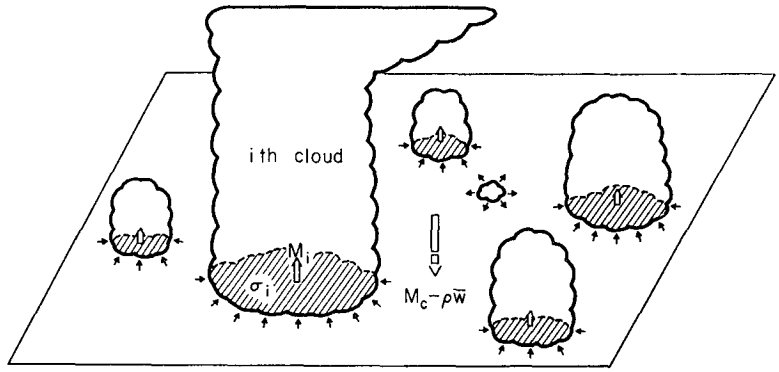

FIG. 1. A unit horizontal area at some level between cloud base and the highest cloud top. The taller clouds are shown penetrating this level and entraining environmental air. A cloud which has lost buoyancy is shown detraining cloud air into the environment.

1971a, b; Yanai *et al.*, 1973). The cumulus convection modifies the large-scale temperature and moisture fields through detrainment and cumulus-induced subsidence in the environment. The detrainment causes large-scale cooling and moistening, and the cumulus-induced subsidence causes large-scale warming and drying. Using a cumulus ensemble model similar to the one presented in Sections 2 and 3 of this paper, Yanai *et al.* (1973) quantitatively derived these effects from observations at a large-scale network of stations. Their results show the importance of the coexistence of shallow clouds with deep clouds in maintaining the large-scale heat and moisture budgets. This agrees with the results obtained with an early version of the UCLA general circulation model, which used a parameterization (Arakawa, 1969) in which there was only a single cloud type at a given time and place. Simulations of the general circulation with that parameterization produced an excessively dry lower troposphere in the regions of deep cumulus convection.

Ooyama (1971) recently developed a cumulus parameterization theory which takes into account the coexistence of clouds of different sizes. He assumed that cumulus clouds can be represented as non-interacting spherical bubbles, dispatched from below. He concluded that the problem of parameterization of cumulus convection reduces to a determination of the dispatcher function. However, the determination of the dispatcher function was left as an open question, so that the parameterization was not closed.

This paper presents a closed theory of the mutual interaction of a cumulus cloud ensemble with the large-scale environment. The theory includes a formulation of the way in which the cloud ensemble is controlled by the large-scale fields. The control mechanism is formulated as a large-scale forcing, which is a destabilizing effect by large-scale processes both above and within the subcloud mixed layer.

The basis of the theory is a quasi-equilibrium of the cloud work function, which is an integral measure of the buoyancy force of the cumulus clouds defined for each cloud type. This concept of quasi-equilibrium, originally proposed by Arakawa (1969), provides a closure condition on the parameterization.

2. Modification of the large-scale environment by cumulus clouds

Consider a horizontal area at some level between cloud base and the highest cloud top. This horizontal area, which we designate as our unit horizontal area, is shown schematically in Fig. 1. It must be large enough to contain an ensemble of cumulus clouds but small enough to cover only a fraction of a large-scale disturbance. The existence of such an area is one of the basic assumptions of this paper.

Because we are not concerned here with acoustic waves, the mass continuity equation can be simplified to its quasi-Boussinesq form

$$\nabla\cdot(\rho\mathbf{v})+\frac{\partial}{\partial z}(\rho w)=0, \tag{1}$$

where the density ρ is a function of height only, $\mathbf{v}$ is the horizontal velocity, ∇ the horizontal del operator, w the vertical velocity, and z the vertical coordinate.

Let $\sigma_i(z,t)$ be the fractional area covered by the ith cloud, in a horizontal cross section at level z and time t. The vertical mass flux through σ_i is

$$M_i=\int_{\sigma_i}\rho w d\sigma=\rho\sigma_i w_i, \tag{2}$$

where

$$\int_{\sigma_i} d\sigma$$

is the integral over the area σ_i and w_i the average vertical velocity of the ith cloud at this level.

The inward mass flux per unit height, normal to the lateral boundary of the ith cloud, is given by $\partial M_i/\partial z$

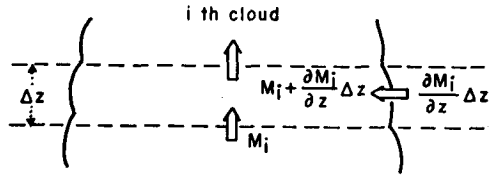

FIG. 2. A schematic diagram of the mass continuity for a thin layer in the ith cloud.

from the mass continuity equation (1) (see Fig. 2). Here the boundary is not necessarily vertical. Then the mass added to the cloud, which may be horizontally expanding or shrinking, is $\partial M_i/\partial z+\rho\partial\sigma_i/\partial t$ per unit height and unit time. The entrainment and detrainment of mass are given by

Entrainment:

$$E_i=\left(\frac{\partial M_i}{\partial z}+\rho\frac{\partial\sigma_i}{\partial t}\right), \quad \text{when} \quad \frac{\partial M_i}{\partial z}+\rho\frac{\partial\sigma_i}{\partial t}>0 \tag{3}$$

Detrainment:

$$D_i=-\left(\frac{\partial M_i}{\partial z}+\rho\frac{\partial\sigma_i}{\partial t}\right), \quad \text{when} \quad \frac{\partial M_i}{\partial z}+\rho\frac{\partial\sigma_i}{\partial t}<0. \tag{4}$$

E_i can be rewritten as $\sigma_i\partial(\rho w_i)/\partial z+\rho(\partial/\partial t+w_i\partial/\partial z)\sigma_i$. Thus, an entrainment of mass, which is caused by turbulent mixing at the cloud boundary, appears either as a vertical divergence of the mass flux within the cloud, as a horizontal expansion of the cloud as it rises, or as a combination of these, depending on the dynamics of the cloud.

The total vertical mass flux by all of the clouds in the ensemble is

$$M_c=\sum_i M_i, \tag{5}$$

where $\sum_i$ denotes the summation over all clouds which are penetrating the level being considered.

Let $\rho\bar{w}$ be the net vertical mass flux over the large-scale unit horizontal area. It satisfies the continuity equation

$$\overline{\nabla\cdot(\rho\mathbf{v})}+\frac{\partial}{\partial z}(\rho\bar{w})=0, \tag{6}$$

where the bar denotes the average over the unit horizontal area. In general, the total vertical mass flux M_c in the clouds is not the same as the large-scale net vertical mass flux $\rho\bar{w}$. The difference between M_c and $\rho\bar{w}$ is equal to the downward mass flux between the clouds, i.e.,

$$-\tilde{M}=M_c-\rho\bar{w}. \tag{7}$$

With sufficiently intense cumulus activity, M_c can exceed $\rho\bar{w}$ and subsidence (negative $\tilde{M}$) appears in the environment, as in Fig. 1.

At a given height, some clouds may be detraining while other clouds are entraining (see Fig. 1). We define total entrainment E and total detrainment D, at each level, by

$$E=\sum_{\text{e.c.}} E_i, \tag{8}$$

$$D=\sum_{\text{d.c.}} D_i. \tag{9}$$

Here $\sum_{\text{e.c.}}$ denotes the summation over all clouds which are entraining at that level, and $\sum_{\text{d.c.}}$ the summation over all clouds which are detraining at that level; E and D, as well as M_c, are functions of z. From (3), (4), (5), (8) and (9), we obtain

$$E-D=\frac{\partial M_c}{\partial z}+\rho\frac{\partial\sigma_c}{\partial t}, \tag{10}$$

where

$$\sigma_c\equiv\sum_i\sigma_i \tag{11}$$

is the total fractional area covered by all the clouds of the ensemble.

We define the static energy by

$$s=c_pT+gz, \tag{12}$$

where c_p is the specific heat of air under constant pressure, T the temperature, and g gravity; c_pT is the specific enthalpy of the air, and gz is its geopotential per unit mass. The static energy s is approximately conserved by the individual air parcel during dry adiabatic processes. Hydrostatic balance, which we assume for the environment, gives

$$\frac{\partial s}{\partial z}=c_p\left(\frac{p}{p_0}\right)^{R/c_p}\frac{\partial\theta}{\partial z}, \tag{13}$$

where p is pressure, p_0 a standard pressure, R the gas constant, and $\theta\equiv(p_0/p)^{R/c_p}T$ the potential temperature.

From the budgets of static energy and water vapor in the environment, we obtain

$$\frac{\partial}{\partial t}[(1-\sigma_c)\rho\tilde{s}]=-\overline{\nabla\cdot(\rho\mathbf{v}s)}-E\tilde{s}+\sum_{\text{d.c.}}D_is_{Di}-\frac{\partial}{\partial z}(\tilde{M}\tilde{s})-L\mathcal{E}+\tilde{Q}_R, \tag{14}$$

$$\frac{\partial}{\partial t}[(1-\sigma_c)\rho\tilde{q}]=-\overline{\nabla\cdot(\rho\mathbf{v}q)}-E\tilde{q}+\sum_{\text{d.c.}}D_iq_{Di}-\frac{\partial}{\partial z}(\tilde{M}\tilde{q})+\mathcal{E}, \tag{15}$$

where the bar denotes the average over the large-scale horizontal unit area, the tilde denotes the value in the environment (which is assumed to be horizontally

homogeneous for all of the variables), and the subscript D_i denotes the value in the detraining air from the ith cloud; L is the latent heat per unit mass of water vapor, $\mathcal{E}$ the evaporation of the liquid water detrained from the clouds per unit height, $\tilde{Q}_R$ the radiational heating of the environment per unit height, and q the mixing ratio of water vapor. The first three terms on the right in (14) and (15) come from the horizontal area integrations of $-\nabla\cdot(\rho\mathbf{v}s)$ and $-\nabla\cdot(\rho\mathbf{v}q)$ over the environment. The terms $-\partial(\tilde{M}\tilde{s})/\partial z$ and $-\partial(\tilde{M}\tilde{q})/\partial z$ represent the vertical flux convergences in the environment.

Using (10), (9), (7) and (6), Eqs. (14) and (15) may be rewritten as

$$(1-\sigma_c)\rho\frac{\partial\tilde{s}}{\partial t}=\sum_{\text{d.c.}} D_i(s_{D_i}-\tilde{s})-L\mathcal{E}-\tilde{M}\frac{\partial\tilde{s}}{\partial z}$$
$$-[\overline{\nabla\cdot(\rho\mathbf{v}s)}-\overline{\nabla\cdot(\rho\mathbf{v})}\tilde{s}]+\tilde{Q}_R, \quad (16)$$

$$(1-\sigma_c)\rho\frac{\partial\tilde{q}}{\partial t}=\sum_{\text{d.c.}} D_i(q_{D_i}-\tilde{q})+\mathcal{E}-\tilde{M}\frac{\partial\tilde{q}}{\partial z}$$
$$-[\overline{\nabla\cdot(\rho\mathbf{v}q)}-\overline{\nabla\cdot(\rho\mathbf{v})}\tilde{q}]. \quad (17)$$

To simplify Eqs. (16) and (17), we use the empirical fact that the total fractional area covered by active clouds is small compared to unity (see, e.g., Malkus *et al.*, 1961). This is consistent with the theoretical finding, first obtained by Bjerknes (1938), that conditional instability favors the smallest possible horizontal cross section for the saturated rising motion (and the largest possible horizontal cross section for the unsaturated sinking motion) if there is neither friction nor entrainment. Asai and Kasahara (1967) found that cumulus convection most efficiently transports heat upward, and therefore most efficiently releases kinetic energy, when the fractional horizontal area of the rising motion is of the order of several percent. It seems that

$$\sigma_c\ll 1 \quad (18)$$

is an acceptable first approximation.

By definition,

$$\bar{s}=(1-\sigma_c)\tilde{s}+\sum_i \sigma_i s_i, \quad (19)$$

$$\bar{q}=(1-\sigma_c)\tilde{q}+\sum_i \sigma_i q_i, \quad (20)$$

and using (11),

$$\bar{s}=\tilde{s}+\sum_i (s_i-\tilde{s})\sigma_i, \quad (21)$$

$$\bar{q}=\tilde{q}+\sum_i (q_i-\tilde{q})\sigma_i, \quad (22)$$

where $(s_i-\tilde{s})$ and $(q_i-\tilde{q})$ are the excess static energy and the excess mixing ratio of water vapor over the environmnetal values in the ith cloud. Using the approximation (18) and the empirical fact that the temperature difference between the cloud and the environment is small, or $\max(s_i-\tilde{s})\ll\tilde{s}$, we obtain, from (21),

$$\bar{s}\approx\tilde{s}. \quad (23)$$

However, the corresponding inequality, $\max(q_i-\tilde{q})\ll\tilde{q}$, holds only when the environment is near saturation. Therefore, we use $\max(q_i-\tilde{q}^*)\ll\tilde{q}^*$, where $\tilde{q}^*$ is the saturation mixing ratio of water vapor in the environment. Using this in (22), we obtain

$$\bar{q}\approx\tilde{q}+(\tilde{q}^*-\tilde{q})\sigma_c,$$
$$=\tilde{q}\left[1+\frac{1-r}{r}\sigma_c\right], \quad (24)$$

where r is the relative humidity of the environment, $\tilde{q}/\tilde{q}^*$. When $r\gg\sigma_c/(1+\sigma_c)\approx\sigma_c$, that is, when the environment is not extremely dry, the second term in the bracket of (24) can be neglected. Then,

$$\bar{q}\approx\tilde{q}. \quad (25)$$

We further assume that

$$\overline{\nabla\cdot(\rho\mathbf{v})}\approx\nabla\cdot(\rho\bar{\mathbf{v}}), \quad (26)$$

$$\overline{\nabla\cdot(\rho\mathbf{v}s)}\approx\nabla\cdot(\rho\bar{\mathbf{v}}\bar{s}), \quad (27)$$

$$\overline{\nabla\cdot(\rho\mathbf{v}q)}\approx\nabla\cdot(\rho\bar{\mathbf{v}}\bar{q}). \quad (28)$$

Here the bar on the right-hand sides denotes a running horizontal space average, on the scale of the unit area, and not the average within the fixed area. The approximations (26)–(28) are valid when the net lateral horizontal transports across the boundary of the fixed large-scale area by cumulus convection (the horizontal cumulus eddy transports) are negligible compared to the horizontal transports by the large-scale motion.

Using the approximations (18), (23) and (25)–(28), Eqs. (16) and (17) may be rewritten as

$$\rho\frac{\partial\bar{s}}{\partial t}=\sum_{\text{d.c.}} D_i(s_{D_i}-\bar{s})-L\mathcal{E}-\tilde{M}\frac{\partial\bar{s}}{\partial z}-\rho\bar{\mathbf{v}}\cdot\nabla\bar{s}+\tilde{Q}_R, \quad (29)$$

$$\rho\frac{\partial\bar{q}}{\partial t}=\sum_{\text{d.c.}} D_i(q_{D_i}-\bar{q})+\mathcal{E}-\tilde{M}\frac{\partial\bar{q}}{\partial z}-\rho\bar{\mathbf{v}}\cdot\nabla\bar{q}, \quad (30)$$

where $\partial\bar{s}/\partial z$ is a measure of the static stability of the environment [see (13) and (23)], which is usually positive, and $-\tilde{M}\partial\bar{s}/\partial z$ represents the adiabatic warming of the environment when $\tilde{M}<0$ (and cooling when $\tilde{M}>0$) due to the vertical motion. For $\partial\bar{q}/\partial z<0$ (the normal condition), $-\tilde{M}\partial\bar{q}/\partial z$ represents the drying of the environment when $\tilde{M}<0$ (and moistening when $\tilde{M}>0$) due to the vertical motion. From (7), $\tilde{M}$ is given by $-M_c+\rho\bar{w}$.

In addition to the detrainment and evaporation terms, cumulus clouds modify the environment through the cumulus-induced subsidence, $-M_c$, in the environ-

ment. The latent heat released within the clouds does not directly warm the environment, but it maintains the buoyancy of the clouds against the adiabatic cooling due to the upward motion and the cooling produced by the entrainment of drier and colder air from the environment. Thus, the latent heat released within the clouds maintains the vertical mass flux of the clouds and, thereby, the cumulus-induced subsidence in the environment. The drying and warming of the environment, by the cumulus-induced subsidence, are the indirect effects of condensation and release of latent heat, but their vertical distributions can be very different from the vertical distribution of the condensation within the clouds. This important role of the cumulus-induced subsidence in the environment was explicitly used for the first-time in parameterizing cumulus convection by Arakawa (1969).[2]

Eqs. (29) and (30) were derived from budgets for the environment only. But they approximately govern the time changes of $\bar{s}$ and $\bar{q}$, which are averages over the total area. This means that the prediction of the large-scale field is practically the same as the prediction of the cloud environment, insofar as the thermodynamic variables are concerned. This important simplification, which was used in the earlier parameterizations by Arakawa (1969, 1972) and by Ooyama (1971), comes from the neglect of accumulative storage of the static energy and water vapor in the ensemble of clouds. In fact, we can rederive the right-hand sides of (29) and (30), as was done by Yanai *et al.* (1973), from budgets for the total area. These budgets give

$$\rho\frac{\partial\bar{s}}{\partial t}=-\overline{\nabla\cdot(\rho\mathbf{v}s)}-\frac{\partial}{\partial z}(\overline{\rho ws})+L(\sum_i C_i-\mathcal{E})+(\sum_i Q_{Ri}+\bar{Q}_R), \quad (31)$$

$$\rho\frac{\partial\bar{q}}{\partial t}=-\overline{\nabla\cdot(\rho\mathbf{v}q)}-\frac{\partial}{\partial z}(\overline{\rho wq})-(\sum_i C_i-\mathcal{E}), \quad (32)$$

where C_i and Q_{R_i} are the rates of condensation of water vapor and radiational heating per unit height in the ith cloud. Using the approximations (27), (28), (26), and Eq. (6), (31) and (32) can be rewritten as

$$\rho\frac{\partial\bar{s}}{\partial t}=-\frac{\partial}{\partial z}[\overline{\rho ws}-\rho\bar{w}\bar{s}]+L(\sum_i C_i-\mathcal{E})+\sum_i Q_{Ri}-\rho\bar{\mathbf{v}}\cdot\nabla\bar{s}-\rho\bar{w}\frac{\partial\bar{s}}{\partial z}+\bar{Q}_R, \quad (33)$$

$$\rho\frac{\partial\bar{q}}{\partial t}=-\frac{\partial}{\partial z}[\overline{\rho wq}-\rho\bar{w}\bar{q}]-(\sum_i C_i-\mathcal{E})-\rho\bar{\mathbf{v}}\cdot\nabla\bar{q}-\rho\bar{w}\frac{\partial\bar{q}}{\partial z}. \quad (34)$$

[2] A description of this parameterization was given by Haltiner (1971, p. 188).

The quantities inside the brackets are the eddy vertical transports by cumulus convection. The eddy transport of s may be written as

$$\overline{\rho ws}-\rho\bar{w}\bar{s}=(\sum_i M_i s_i+\tilde{M}\tilde{s})-\rho\bar{w}\bar{s}.$$

Using (7), (19), (11) and (2), the eddy transport can be rewritten as

$$\overline{\rho ws}-\rho\bar{w}\bar{s}=\sum_i \rho\sigma_i[w_i(s_i-\bar{s})-\tilde{w}(s_i-\tilde{s})],$$

where $\tilde{w}$ is the vertical velocity in the environment. The second term in the bracket is negligible compared to the first, since $w_i\gg|\tilde{w}|$ and $s_i-\bar{s}\approx s_i-\tilde{s}$. Therefore

$$\overline{\rho ws}-\rho\bar{w}\bar{s}\approx\sum_i M_i(s_i-\bar{s}). \quad (35)$$

Similarly, the eddy transport of q may be rewritten as

$$\overline{\rho wq}-\rho\bar{w}\bar{q}\approx\sum_i M_i(q_i-\bar{q}). \quad (36)$$

When there are no accumulative storages of mass, static energy and water vapor in the cloud ensemble,

$$E-D-\frac{\partial M_c}{\partial z}=0, \quad (37)$$

$$E\bar{s}-\sum_{\text{d.e.}} D_i s_{Di}-\frac{\partial}{\partial z}\sum_i M_i s_i+L\sum_i C_i+\sum_i Q_{Ri}=0, \quad (38)$$

$$E\bar{q}-\sum_{\text{d.e.}} D_i q_{Di}-\frac{\partial}{\partial z}\sum_i M_i q_i-\sum_i C_i=0. \quad (39)$$

Using (35)–(39), we can easily show that (33) and (34) are identical to (29) and (30), where the heat of condensation and the radiational heating in the clouds do not explicitly appear.

If we assume that the evaporation of the detrained liquid water takes place at the same level where the water is detrained from the clouds, then

$$\mathcal{E}=\sum_{\text{d.e.}} D_i l_{Di}, \quad (40)$$

where l_{Di} is the mixing ratio of liquid water in the air detrained from the ith cloud. This assumption is probably justifiable for the detrained cloud droplets, but not for any large raindrops that might be detrained from the clouds. With the assumption (40) and Eq. (7), (29) and (30) can be rewritten as

$$\rho\frac{\partial\bar{s}}{\partial t}=\sum_{\text{d.e.}} D_i[(s-Ll)_{Di}-\bar{s}]+M_c\frac{\partial\bar{s}}{\partial z}-\rho\bar{\mathbf{v}}\cdot\nabla\bar{s}-\rho\bar{w}\frac{\partial\bar{s}}{\partial z}+\bar{Q}_R, \quad (41)$$

$$\rho\frac{\partial\bar{q}}{\partial t}=\sum_{\text{d.c.}}D_i[(q+l)_{Di}-\bar{q}]+M_c\frac{\partial\bar{q}}{\partial z}-\rho\bar{\mathbf{v}}\cdot\nabla\bar{q}-\rho\bar{w}\frac{\partial\bar{q}}{\partial z}. \quad (42)$$

The detrainment terms will be further simplified in the next section.

3. Budget equations for an individual cloud and assumptions on detrainment

We first consider the budgets of mass, static energy, water vapor, and liquid water for an individual cloud. In the entrainment layer of the ith cloud, the budget equations can be written as

Mass:

$$\frac{\partial}{\partial t}(\rho\sigma_i)=E_i-\frac{\partial}{\partial z}M_i \quad (43)$$

Static energy:

$$\frac{\partial}{\partial t}(\rho\sigma_i s_i)=E_i\bar{s}-\frac{\partial}{\partial z}(M_i s_i)+LC_i+Q_{Ri} \quad (44)$$

Water vapor:

$$\frac{\partial}{\partial t}(\rho\sigma_i q_i)=E_i\bar{q}-\frac{\partial}{\partial z}(M_i q_i)-C_i \quad (45)$$

Liquid water:

$$\frac{\partial}{\partial t}(\rho\sigma_i l_i)=-\frac{\partial}{\partial z}(M_i l_i)+C_i-R_i. \quad (46)$$

Here l_i is the mixing ratio of liquid water in the form of cloud droplets and R_i the rate of conversion of the liquid water to precipitation per unit height. The approximations (23) and (25) have already been used. The budget equations in the detrainment layer are

Mass:

$$\frac{\partial}{\partial t}(\rho\sigma_i)=-D_i-\frac{\partial}{\partial z}M_i \quad (47)$$

Static energy:

$$\frac{\partial}{\partial t}(\rho\sigma_i s_i)=-D_i s_{Di}-\frac{\partial}{\partial z}(M_i s_i)+LC_i+Q_{Ri} \quad (48)$$

Water vapor:

$$\frac{\partial}{\partial t}(\rho\sigma_i q_i)=-D_i q_{Di}-\frac{\partial}{\partial z}(M_i q_i)-C_i \quad (49)$$

Liquid water:

$$\frac{\partial}{\partial t}(\rho\sigma_i l_i)=-D_i l_{Di}-\frac{\partial}{\partial z}(M_i l_i)+C_i-R_i. \quad (50)$$

Eqs. (37)–(39) can be obtained by summation of (43)–(45) over all entraining clouds, and of (47)–(49) over all detraining clouds, and by subsequent dropping of the time derivative terms.

Eliminating C_i from (44) and (45) and from (45) and (46), we obtain

$$\frac{\partial}{\partial t}(\rho\sigma_i h_i)=E_i\bar{h}-\frac{\partial}{\partial z}(M_i h_i)+Q_{Ri}, \quad (51)$$

$$\frac{\partial}{\partial t}[\rho\sigma_i(q+l)_i]=E_i\bar{q}-\frac{\partial}{\partial z}[M_i(q+l)_i]-R_i, \quad (52)$$

where the moist static energy h is defined by

$$h\equiv s+Lq\equiv c_pT+gz+Lq. \quad (53)$$

The moist static energy is approximately conserved by an individual air parcel during moist adiabatic processes. Eqs. (51) and (52) describe the budgets of the moist static energy and water substance for the entrainment layer of the ith cloud.

We assume that the air is saturated in the clouds. Then $q_i=q^*(T_i,p_i)$, where the asterisk denotes the saturation value. If the effect on q^* of a pressure difference between the cloud and the environment is neglected,[3] then

$$q_i\approx q^*(T_i,\bar{p}),$$

$$\approx\bar{q}^*+\frac{1}{c_p}\left(\frac{\partial\bar{q}^*}{\partial\bar{T}}\right)_{\bar{p}}(s_i-\bar{s}). \quad (54)$$

Here $\bar{q}^*\equiv q^*(\bar{T},\bar{p})$, and

$$s_i-\bar{s}\approx\frac{1}{1+\gamma}(h_i-\bar{h}^*), \quad (55)$$

$$q_i-\overline{q^*}\approx\frac{\gamma}{1+\gamma}\frac{1}{L}(h_i-\bar{h}^*), \quad (56)$$

where

$$\gamma\equiv\frac{L}{c_p}\left(\frac{\partial\bar{q}^*}{\partial\bar{T}}\right)_{\bar{p}}. \quad (57)$$

The symbol $\bar{h}^*\equiv\bar{s}+L\bar{q}^*$ is the saturation value of moist static energy of the environment; $\partial\overline{h^*}/\partial z\gtrless 0$ defines, respectively, the moist adiabatically stable, neutral, and unstable lapse rates of the environment.

The ith cloud may be in its growing stage, with a rising cloud top. We then assume that there is entrainment into the cloud at all levels including the cloud top. Only after the cloud top has reached its maximum height and has stopped rising does detrainment take place in a

[3] Although the scale analysis by Ogura and Phillips (1962) did not justify this approximation, the recent numerical integration by Wilhelmson and Ogura (1972) indicates that the pressure difference was overestimated by the scale analysis.

thin layer at the cloud top. We further assume that the maximum height of the cloud top is approximately equal to the height of the vanishing buoyancy level.[4]

The sign of the buoyancy is determined by the excess of the virtual static energy in the cloud over the environmental value. The virtual static energy is approximately given by

$$s_v = s + c_p\bar{T}(\delta q - l), \tag{58}$$

where $\delta = 0.608$. The excess virtual static energy is

$$s_{v_i} - \bar{s}_v = s_i - \bar{s} + c_p\bar{T}[\delta(q_i - \bar{q}) - l_i]. \tag{59}$$

The level $\hat{z}_i$, at which the cloud top loses buoyancy, is given by

$$(s_{v_i} - \bar{s}_v)_{z=\hat{z}_i} = 0, \tag{60}$$

or, from (59),

$$\{s_i - \bar{s} + c_p\bar{T}[\delta(q_i - \bar{q}) - l_i]\}_{z=\hat{z}_i} = 0. \tag{61}$$

Let us assume that all clouds which lose buoyancy at the same level z have a common value $\hat{l}$ for l_i at that level. Then,

$$(l_i - \hat{l})_{z=\hat{z}_i} = 0. \tag{62}$$

We let $\hat{l}$ be a function of z, where $\hat{l}$ at different levels is for different types of clouds. Although $\hat{l}$ is the liquid water mixing ratio at the level of vanishing buoyancy, it is not necessarily equal to the liquid water mixing ratio of the air which spreads into the environment, because an additional condensation (or evaporation) may be taking place near the cloud top due to concentrated radiational cooling (or heating) there.

Use of (55), (56) and (62), with the vanishing buoyancy condition (61), gives

$$(h_i - \hat{h}^*)_{z=\hat{z}_i} = 0, \tag{63}$$

where

$$\hat{h}^* \equiv \bar{h}^* - \frac{(1+\gamma)L\epsilon}{1+\gamma\epsilon\delta}[\delta(\bar{q}^* - \bar{q}) - \hat{l}], \tag{64}$$

and $\epsilon \equiv c_p\bar{T}/L$.

For the detrainment layer, it is convenient to eliminate C_i from (48) and (50). Then we have

$$\frac{\partial}{\partial t}[\rho\sigma_i(s - Ll)_i] = -D_i(s - Ll)_{Di} - \frac{\partial}{\partial z}[M_i(s - Ll)_i] + LR_i + Q_{Ri}. \tag{65}$$

We also have the budget equation for water substance

$$\frac{\partial}{\partial t}[\rho\sigma_i(q + l)_i] = -D_i(q + l)_{Di} - \frac{\partial}{\partial z}[M_i(q + l)_i] - R_i. \tag{66}$$

Because the thickness of the detrainment layer, Δz_{Di}, is assumed to be small, the mass budget equation (47) for the detrainment layer may be approximated by

$$D_i\Delta z_{Di} = (M_i)_{z=\hat{z}_i}, \tag{67}$$

where M_i at $z = \hat{z}_i$ is the mass flux of the cloud entering the detrainment layer from below. Similar simplifications of (65) and (66), and use of (67) give

$$D_i(s - Ll)_{Di} = D_i[(s - Ll)_i]_{z=\hat{z}_i} + Q_{Ri}, \tag{68}$$

$$D_i(q + l)_{Di} = D_i[(q + l)_i]_{z=\hat{z}_i}. \tag{69}$$

The radiation term in (68) is retained because $Q_{Ri}\Delta z_{Di}$ is finite even when Δz_{Di} is infinitesimally small.

Use of (55), (56), (62), (63) and (64) in (68) and (69) gives

$$\sum_{\text{d.c.}} D_i(s - Ll)_{Di} = D(\hat{s} - L\hat{l}) + \sum_{\text{d.c.}} Q_{Ri}, \tag{70}$$

$$\sum_{\text{d.c.}} D_i(q + l)_{Di} = D(\hat{q}^* + \hat{l}), \tag{71}$$

where D is the total detrainment $\sum_{\text{d.c.}} D_i$ and

$$\hat{s} \equiv \bar{s} - \frac{L\epsilon}{1+\gamma\epsilon\delta}[\delta(\bar{q}^* - \bar{q}) - \hat{l}], \tag{72}$$

$$\hat{q}^* \equiv \bar{q}^* - \frac{\gamma\epsilon}{1+\gamma\epsilon\delta}[\delta(\bar{q}^* - \bar{q}) - \hat{l}]. \tag{73}$$

Substituting (70) and (71) into (41) and (42), we obtain

$$\rho\frac{\partial\bar{s}}{\partial t} = D(\hat{s} - \bar{s} - L\hat{l}) + M_c\frac{\partial\bar{s}}{\partial z} - \rho\bar{\mathbf{v}}\cdot\nabla\bar{s} - \rho\bar{w}\frac{\partial\bar{s}}{\partial z} + \bar{Q}_R, \tag{74}$$

where

$$\bar{Q}_R \equiv \tilde{Q}_R + \sum_{\text{d.c.}} Q_{Ri}, \tag{74}'$$

and

$$\rho\frac{\partial\bar{q}}{\partial t} = D(\hat{q}^* + \hat{l} - \bar{q}) + M_c\frac{\partial\bar{q}}{\partial z} - \rho\bar{\mathbf{v}}\cdot\nabla\bar{q} - \rho\bar{w}\frac{\partial\bar{s}}{\partial z}. \tag{75}$$

Note that $\bar{Q}_R$ appears in (74), whereas $\tilde{Q}_R$ appears in (41). These are the basic equations we use to describe the time changes of the large-scale temperature and moisture fields. Similar equations were derived for a three-level model of the large-scale temperature and moisture fields by Arakawa (1969), and for the continuous atmosphere by Ooyama (1971), Arakawa (1971) and Yanai (1971b). Yanai *et al.* (1973) used these equations to determine the bulk properties of tropical cumulus cloud clusters from the observed large-scale budgets of heat and moisture. In that study, the large-scale tendency terms were given from observations. But our problem is a prognostic one, and the large-scale tendency terms are precisely what we wish to obtain from the parameterization of cumulus convection.

[4] The conventional assumption that a cumulus cloud ceases vertical growth when its temperature sounding recrosses the environment curve is supported by the cloud model of Simpson *et al.* (1965).

4. Spectral representation of the cumulus ensemble

Eqs. (74) and (75) show which properties of the cumulus ensemble must be found to predict the large-scale temperature and moisture fields. The modification of the large-scale fields by cumulus convection depends on 1) the total mass flux in the clouds, $M_c(z)$, 2) the total detrainment from the clouds into the environment, $D(z)$, and 3) the mixing ratio of liquid water at the vanishing buoyancy level, $\hat{l}(z)$. Therefore, the problem of parameterization of cumulus convection has reduced to relating these properties of the cumulus ensemble to the large-scale temperature, moisture and velocity fields. (In addition, cumulus clouds modify the large-scale temperature through $\sum_{\text{d.c.}} Q_{Ri}$, the radiational heating.)

The total detrainment $D(z)$ at different levels refers to different types of clouds. When the thickness of the detrainment layer, Δz_{Di}, is infinitesimally small, the total detrainment in the layer between z and $z+dz$, $D(z)dz$, is equal to the total mass flux, at level z, of the clouds which lose buoyancy within that layer. It is now clear that finding the total detrainment $D(z)$, as a function of height, is equivalent to finding the distribution of the mass flux in the different types of clouds which lose buoyancy at the different levels. This suggests that we represent the cloud ensemble in spectral form, by dividing the ensemble into sub-ensembles, each of which has a characteristic cloud type.

For simplicity, we assume that a single positive parameter λ can fully characterize a cloud type. Then the detrainment level z_D, which is the maximum height of the cloud top, becomes a function of λ. We will choose λ so that $z_D(\lambda)$ will decrease as λ increases, as shown schematically in Fig. 3. A more specific definition of λ will be given later. Let $\lambda_D(z)$ be the λ of the clouds which are detraining at level z. Then $\lambda_D(z)$ is the inverse function of $z_D(\lambda)$, which satisfies

$$z \equiv z_D[\lambda_D(z)] \tag{76}$$

identically; and $\lambda_D(z)$ is the maximum value of λ at level z, because the clouds which have λ larger than λ_D have detrainment levels lower than z.

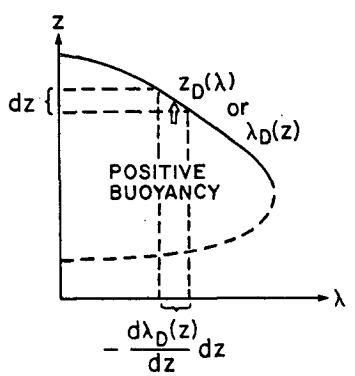

FIG. 3. The detrainment level z_D as a function of λ, or λ_D of the detraining clouds as a function of z.

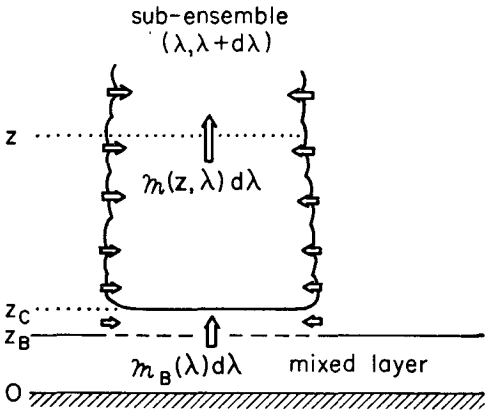

FIG. 4. A schematic diagram which shows the sub-ensemble of type λ clouds and the subcloud mixed layer. The updraft, which originates in the mixed layer, is unsaturated in the region between z_C and z_B.

The total mass flux in the clouds, M_c, can be expressed as

$$M_c(z) = \int_0^{\lambda_D(z)} \mathfrak{M}(z,\lambda)d\lambda, \tag{77}$$

where

$$\mathfrak{M}(z,\lambda)d\lambda = \sum_{\lambda_i \in (\lambda,\lambda+d\lambda)} M_i(z) \tag{78}$$

is the sub-ensemble mass flux due to the clouds which have the parameter λ_i in the interval $(\lambda, \lambda+d\lambda)$.

The total detrainment $D(z)dz$ in the layer between z and $z+dz$ is equal to the sub-ensemble mass flux, at level z, due to the clouds which have parameter λ_i in the interval $\lambda_D(z)-(-d\lambda_D(z)/dz)dz$ to $\lambda_D(z)$, as is shown in Fig. 3. Then we have

$$D(z) = -\mathfrak{M}(z,\lambda_D(z))\frac{d\lambda_D(z)}{dz}. \tag{79}$$

It is convenient to normalize $\mathfrak{M}(z,\lambda)$ by

$$\mathfrak{M}(z,\lambda) \equiv \mathfrak{M}_B(\lambda)\eta(z,\lambda), \tag{80}$$

where

$$\mathfrak{M}_B(\lambda) \equiv \mathfrak{M}(z_B,\lambda), \tag{81}$$

and z_B is a properly chosen *base* of the updrafts associated with the clouds. Obviously,

$$\eta(z_B,\lambda) = 1. \tag{82}$$

We shall find it convenient to choose the top of the subcloud mixed layer as the base z_B as shown in Fig. 4. In the next section, we will refer to observations which show that the top of the mixed layer is located somewhat below the cloud base z_C. The vertical mass flux below the cloud base should be interpreted as the mass

flux of the updrafts *associated with* the clouds but not *in* the clouds.

Next, we consider the budgets of mass, moist static energy, and water substance for the sub-ensemble. The summation of (43) over all members of the sub-ensemble, and subsequent dropping of the time derivative term, gives

$$\frac{\partial \eta(z,\lambda)}{\partial z}=\Big[\sum_{\lambda i\epsilon(\lambda,\lambda+d\lambda)} E_i(z)\Big]/[\mathfrak{M}_B(\lambda)d\lambda], \tag{83}$$

where (78) and (80) have been used. Similarly, (51) and (52) give

$$\frac{\partial}{\partial z}[\eta(z,\lambda)h_c(z,\lambda)]=\frac{\partial \eta(z,\lambda)}{\partial z}\bar{h}(z), \tag{84}$$

$$\frac{\partial}{\partial z}\{\eta(z,\lambda)[q_c(z,\lambda)+l(z,\lambda)]\} =\frac{\partial \eta(z,\lambda)}{\partial z}\bar{q}(z)-\eta(z,\lambda)r(z,\lambda), \tag{85}$$

where (78), (80) and (83) have been used. The symbols $h_c(z,\lambda)$, $q_c(z,\lambda)$ and $l(z,\lambda)$ are h, q and l, respectively, in the clouds which are members of the sub-ensemble; and $r(z,\lambda)$ is defined by

$$\mathfrak{M}(z,\lambda)r(z,\lambda)d\lambda\equiv\sum_{\lambda i\epsilon(\lambda,\lambda+d\lambda)} R_i. \tag{86}$$

The radiational heating in the entrainment layer is neglected.

Eqs. (84) and (85) can be rewritten as

$$\frac{\partial h_c(z,\lambda)}{\partial z}=-\mu(z,\lambda)[h_c(z,\lambda)-\bar{h}(z)], \tag{87}$$

$$\frac{\partial}{\partial z}[q_c(z,\lambda)+l(z,\lambda)] =-\mu(z,\lambda)[q_c(z,\lambda)+l(z,\lambda)-\bar{q}(z)]-r(z,\lambda), \tag{88}$$

where $\mu(z,\lambda)$ is the fractional rate of entrainment for the sub-ensemble, given by

$$\mu(z,\lambda)\equiv\frac{1}{\eta(z,\lambda)}\frac{\partial \eta(z,\lambda)}{\partial z}. \tag{89}$$

Except for the dynamical and cloud microphysical processes which determine $r(z,\lambda)$ and the subcloud layer processes which determine $h_c(z_B,\lambda)$ and $q_c(z_B,\lambda)$, the problem of parameterizing cumulus convection has now been reduced to finding the normalized vertical profile of the sub-ensemble mass flux $\eta(z,\lambda)$, and the mass flux distribution function at the top of the mixed layer $\mathfrak{M}_B(\lambda)$. In order to show this, let us assume that $\eta(z,\lambda)$ [and, therefore, $\mu(z,\lambda)$] is known. In this case $h_c(z,\lambda)$ can be readily obtained by integrating (84) or (87) with respect to height, with given $\bar{h}(z)$ and $h_c(z_B,\lambda)$; and $q_c(z,\lambda)$ above cloud base is then obtained by using the saturation condition (56), rewritten in the form

$$q_c(z,\lambda)-\bar{q}^*(z)=\frac{\gamma}{1+\gamma}\frac{1}{L}[h_c(z,\lambda)-\bar{h}^*(z)]. \tag{90}$$

The value of $q_c(z,\lambda)$ below cloud base can be obtained by integrating the water substance budget equation [(85) or (88)] with $l(z,\lambda)=0$, and with given $\bar{q}(z)$ and $q_c(z_B,\lambda)$. Cloud base can be determined by the continuity of $q_c(z,\lambda)$ below cloud base and above cloud base. Above cloud base $q_c(z,\lambda)+l(z,\lambda)$ can be obtained by integrating the water substance equation further upward, with a parameterized $r(z,\lambda)$. Then from the known $q_c(z,\lambda)$ and $q_c(z,\lambda)+l(z,\lambda)$ above cloud base, we can find $l(z,\lambda)$. The liquid water mixing ratio at the vanishing buoyancy level is given by

$$\hat{l}(z)=l[z,\lambda_D(z)], \tag{91}$$

where $\lambda_D(z)$ is the inverse function of $z_D(\lambda)$, and the detrainment level $z_D(\lambda)$ is found from the condition of vanishing buoyancy (63), rewritten in the form

$$h_c[z_D(\lambda),\lambda]=\hat{h}^*[z_D(\lambda)]. \tag{92}$$

Here $\hat{h}^*$ is defined by (64) and

$$\hat{l}[z_D(\lambda)]=l\{z_D(\lambda),\lambda_D[z_D(\lambda)]\}, =l[z_D(\lambda),\lambda]. \tag{93}$$

Then, only the mass flux distribution function $\mathfrak{M}_B(\lambda)$, which is needed for computing $M(z)$ and $D(z)$ from (77) and (79), remains unknown.

Although our knowledge of the dynamics of clouds is far from adequate, the determination of the normalized vertical profile of the sub-ensemble mass flux $\eta(z,\lambda)$ is logically more straightforward than the determination of the mass flux distribution function $\mathfrak{M}_B(\lambda)$. We may assume that the members of a sub-ensemble are at random phases in their life cycle and, therefore, the summation of the mass flux over all members of the sub-ensemble, as in (78), is proportional to the mass flux of a single cloud averaged over its entire lifetime. The constant of proportionality is the number of clouds. But the constant of proportionality does not matter for $\eta(z,\lambda)$, since $\eta(z,\lambda)$ is normalized. A dynamical model which governs the life cycle of a single cloud will determine the vertical profile of the time-averaged mass flux of that cloud and, therefore, will determine $\eta(z,\lambda)$ for each cloud type characterized by parameter λ. But we are assuming that a single scalar parameter λ is sufficient to characterize the cloud type. For this assumption to be approximately valid, we must choose the parameter λ properly.

The one-dimensional model of the cumulus tower, developed by Simpson *et al.* (1965) and Simpson and Wiggert (1969, 1971), has been extensively tested against observations. This model specifies the fractional

rate of entrainment by

$$\mu=\frac{2\alpha}{R}, \tag{94}$$

where R is the radius of the rising cumulus tower and α the entrainment constant (see also Simpson, 1971); R is either measured or assumed at the cloud base and given to the model as an input. The assumption that R is constant with height, in the Lagrangian sense, leads to better agreement with observations than the alternative assumptions of horizontally expanding thermals or starting plumes (Simpson *et al.*, 1965).

In our model, also, we assume that R is constant with height in the Lagrangian sense. We do not assume that the cloud is a column-like steady jet; but we do assume that the fractional rate of entrainment *for the time-averaged mass flux* of the cloud is approximately constant with height. Therefore, the cloud may consist of a sequence of active elements which have a negligible *horizontal* expansion rate below the level of vanishing buoyancy. We choose this constant fractional rate of entrainment as the parameter λ which characterizes the cloud type. Although the dependence of the entrainment on the radius, as given by (94), is not used explicitly, we may interpret the larger λ as representing the smaller clouds and the smaller λ as representing the larger clouds.

The assumption of constant fractional rate of entrainment greatly simplifies the determination of $\eta(z,\lambda)$. This assumption decouples the determination of $\eta(z,\lambda)$, the normalized time-averaged mass flux, from the solution of the entire system of equations which governs the life cycle of a cloud. An assumption about the geometry, such as that of expanding spherical bubbles used by Ooyama (1971), gives a similar simplification.

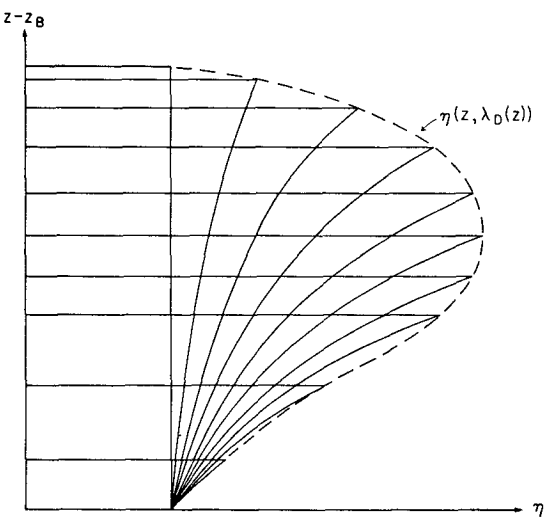

FIG. 5. Schematic profiles of the normalized mass flux $\eta(z,\lambda)$ for various λ. The envelope of these curves is $\eta[z,\lambda_D(z)]$.

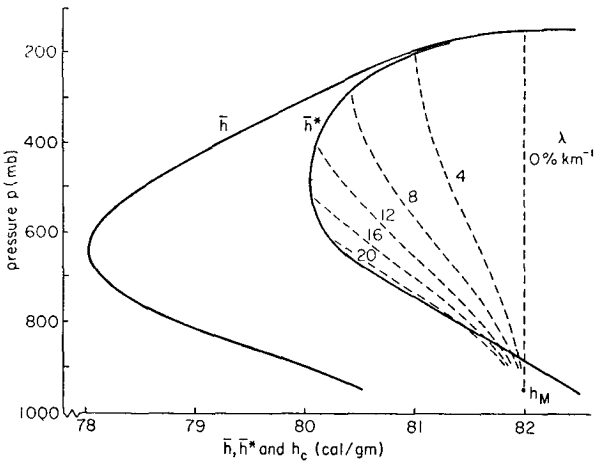

FIG. 6. Vertical profiles of $\bar{h}(p)$, $\bar{h}^*(p)$ and $h_c(p,\lambda)$; $h_c(p,\lambda)$ lines are dashed and labeled with the value of λ in percent per kilometer. Profiles of $\bar{h}$ and $\bar{h}^*$ were obtained from Jordan's (1958) "mean hurricane season" sounding. The top p_B of the mixed layer is assumed to be 950 mb; h_M is assumed to be 82 cal gm^{-1}.

Replacing $\mu(z,\lambda)$ in (89) by λ, we obtain

$$\frac{\partial\eta(z,\lambda)}{\partial z}=\lambda\eta(z,\lambda). \tag{95}$$

Eqs. (95), (82) and the definition of $z_D(\lambda)$ immediately give

$$\eta(z,\lambda)=\begin{cases} e^{\lambda(z-z_B)}, & z_B\leqslant z\leqslant z_D(\lambda) \\ 0, & z_D(\lambda)<z \end{cases}. \tag{96}$$

Thus, the sub-ensemble vertical mass flux increases exponentially with height due to the entrainment. Above the detrainment level $z_D(\lambda)$, the mass flux becomes zero. Fig. 5 schematically shows $\eta(z,\lambda)$ for various λ.

To determine $z_D(\lambda)$, we must find $h_c(z,\lambda)$. The solution of (84) is given by

$$h_c(z,\lambda)=\frac{1}{\eta(z,\lambda)}\left[h_c(z_B,\lambda)+\lambda\int_{z_B}^{z}\eta(z',\lambda)\bar{h}(z')dz'\right]. \tag{97}$$

Here, (95) has been used. Above the condensation level, (55) gives

$$s_c(z,\lambda)-\bar{s}(z)=\frac{1}{1+\gamma(z)}[h_c(z,\lambda)-\bar{h}^*(z)], \tag{98}$$

where γ is defined by (57).[5] As an example, for given $\bar{h}(z)$, $\bar{h}^*(z)$, z_B and a constant $h_c(z_B,\lambda)=h_M$, $h_c(z,\lambda)$ is

[5] Below the condensation level z_C, Eq. (98) must be replaced by

$$s_c(z,\lambda)-\bar{s}(z)=\frac{1}{\eta(z,\lambda)}\left[s_c(z_B,\lambda)+\lambda\int_{z_B}^{z}\eta(z',\lambda)\bar{s}(z')dz'\right]-\bar{s}(z). \tag{98'}$$

The condensation level is obtained by the consistency of (98) with (98') at z_C.

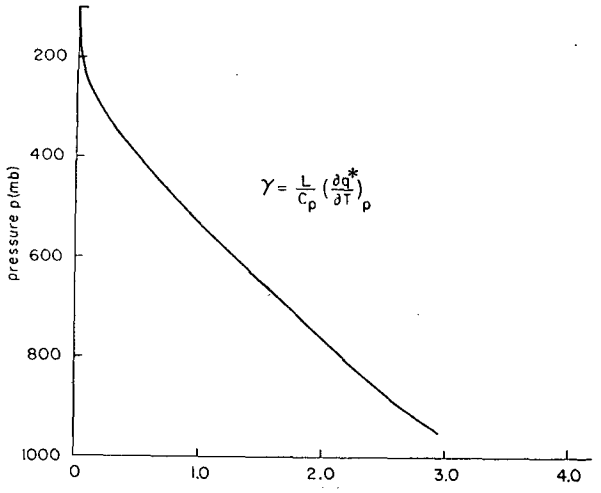

FIG. 7. The function $\gamma(p)$ for Jordan's "mean hurricane season" sounding.

shown by the broken lines in Fig. 6 and $\gamma(z)$ is shown in Fig. 7. In the figures pressure is used as the vertical coordinate. For $\lambda=0$, $\eta(z,0)=1$ and the second term in the bracket of (97) vanishes. Then $h_c(z,0)=h_M$ for all z. As λ increases, $h_c(z,\lambda)$ is more rapidly diluted by $\bar{h}(z)$. When the difference between $\hat{h}^*$ and $\bar{h}^*$ is neglected, the detrainment level is given by the intersections of the broken lines with the curve $\overline{h^*}(z)$ in Fig. 6. The curve $p_D(\lambda)$, the pressure at the detrainment level thus obtained, is shown in Fig. 8. This figure shows that smaller clouds (larger λ) have lower detrainment levels than larger clouds (smaller λ) because smaller clouds, which have a larger entrainment rate, lose positive buoyancy more quickly than larger clouds.

To find the mixing ratio of liquid water, we integrate (85) with respect to height from a given $q_c(z_B, \lambda)$. In addition, a parameterization of the rainfall rate $r(z,\lambda)$ is necessary; a very crude, but perhaps adequate parameterization, is used in Appendix B.

It remains to find the base level variables, z_B, $h_c(z_B,\lambda)$, $q_c(z_B,\lambda)$, and most importantly, the mass flux distribution function, $\mathfrak{M}_B(\lambda)$. Up to this point our theory is not substantially different from that of Ooyama (1971), as far as the basic logic is concerned. Ooyama concluded that the problem of parameterization of cumulus convection reduces to finding a "dispatcher function," the rate of generation of buoyant bubbles as a function of the initial state of the bubbles. However, Ooyama left the determination of this dispatcher function as an open question and because of this his parameterization is not complete.

5. Budgets of static energy and moisture for the mixed layer

In this section we present a model of the subcloud mixed layer which interacts with the cumulus ensemble. Observations over the Caribbean by Bunker *et al.* (1949) and Malkus (1958) show that between the ocean surface and the cloud base level there typically exists a mixed layer in which the potential temperature θ and the mixing ratio of water vapor q, and therefore s and h, are approximately constant with height. The top of the mixed layer is somewhat ($\sim$200 m) lower than the cloud base level. Except for the region directly below the clouds, there typically exists a thin transition layer immediately above the mixed layer in which θ, and therefore s, rapidly increase and q rapidly decreases with height.

We denote the height of the mixed layer by z_B (Fig. 9), where z_B is assumed to be lower than the cloud base z_C, which is approximately the level of lifting condensation. Therefore, we consider here only non-saturated mixed layers.[6] We model the transition layer as a discontinuity in s and q at z_B. In this respect, our approach is similar to those given by Ball (1960), Lilly (1968), Deardorff (1972) and Betts (1973a). We define

$$\Delta s \equiv \bar{s}(z_B+) - s_M, \tag{99}$$

$$\Delta q \equiv \bar{q}(z_B+) - q_M, \tag{100}$$

$$\Delta h \equiv \bar{h}(z_B+) - h_M, \tag{101}$$

where $\bar{s}(z_B+)$, $\bar{q}(z_B+)$ and $\bar{h}(z_B+)$ are values of $\bar{s}$, $\bar{q}$, and $\bar{h}$ evaluated just above the discontinuity at z_B, and s_M, q_M and h_M are the mixed layer values of s, q

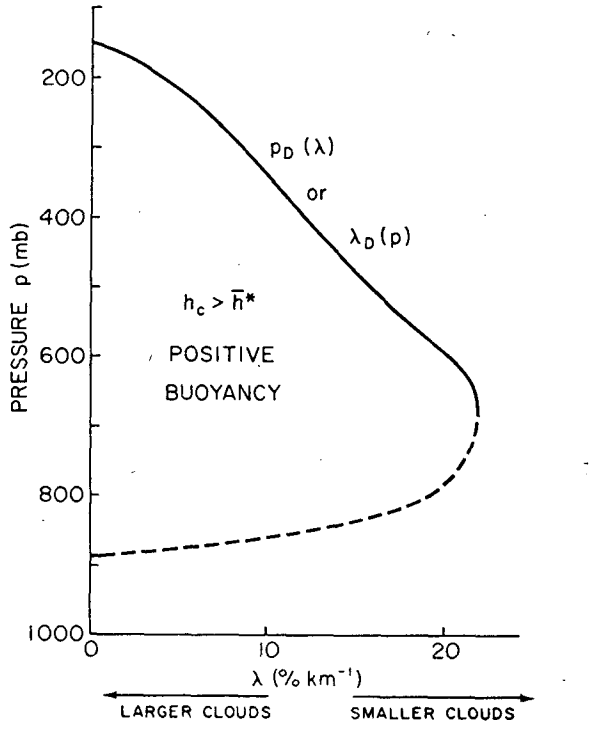

FIG. 8. The function $p_D(\lambda)$ or $\lambda_D(p)$ corresponding to Fig. 6.

[6] Saturated mixed layers will be discussed in a forthcoming paper by Randall and Arakawa (1974).

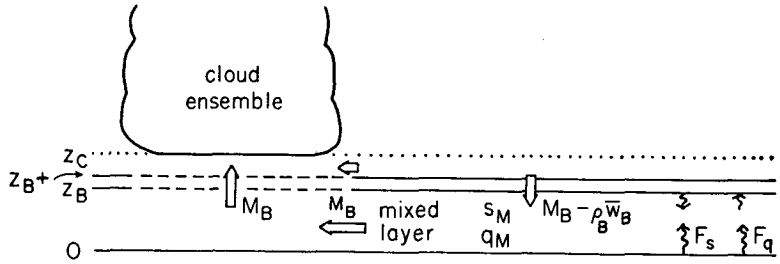

FIG. 9. A schematic diagram of the subcloud mixed layer in which s and q are constant with height. The transition layer (the layer between $z=z_B$ and $z=z_B+$) just above the top of the mixed layer is assumed to be infinitesimally thin and discontinuities in s and q are assumed to occur at z_B. We assume that the mixed layer is unsaturated so that z_C is above z_B. $M_B-\rho_B\bar{w}_B$ is the downward environmental mass flux at z_B. In typical situations the surface turbulent fluxes of s and q are upward, while at z_B the turbulent flux of s is downward and the turbulent flux of q is upward.

and h. The quantity Δh is given by

$$\Delta h=\Delta s+L\Delta q. \tag{102}$$

In typical cumulus situations $L\Delta q$ dominates Δs, making Δh negative. The quantity Δh^* is given by

$$\Delta h^*=[1+\gamma(z_B)]\Delta s, \tag{102}'$$

where γ is defined by (57). Typical vertical profiles of h and h^* near the mixed layer are shown schematically in Fig. 10. Because of the sign of Δh, the cumulus cloud updraft prefers to originate from the mixed layer. In this paper, we shall only treat that type of situation.

In the mixed layer,

$$\rho\frac{\partial s_M}{\partial t}=-\rho\bar{\mathbf{v}}\cdot\nabla s_M-\frac{\partial F_s}{\partial z}+Q_R, \tag{103}$$

$$\rho\frac{\partial q_M}{\partial t}=-\rho\bar{\mathbf{v}}\cdot\nabla q_M-\frac{\partial F_q}{\partial z}, \tag{104}$$

where F_s and F_q are the vertical turbulent eddy fluxes of s and q. Integration of (103) and (104) with respect to z from zero to z_B gives

$$\rho_M\frac{\partial s_M}{\partial t}=-(\rho\bar{\mathbf{v}})_M\cdot\nabla s_M+\frac{1}{z_B}[(F_s)_0-(F_s)_B]+(Q_R)_M, \tag{105}$$

$$\rho_M\frac{\partial q_M}{\partial t}=-(\rho\bar{\mathbf{v}})_M\cdot\nabla q_M+\frac{1}{z_B}[(F_q)_0-(F_q)_B], \tag{106}$$

where

$$\rho_M\equiv\frac{1}{z_B}\int_0^{z_B}\rho dz, \tag{107}$$

$$(\rho\bar{\mathbf{v}})_M\equiv\frac{1}{z_B}\int_0^{z_B}\rho\bar{\mathbf{v}}dz, \tag{108}$$

$$(Q_R)_M\equiv\frac{1}{z_B}\int_0^{z_B}Q_R dz. \tag{109}$$

The terms $(F_s)_0$ and $(F_q)_0$ are the fluxes of s and q at the surface, while $(F_s)_B$ and $(F_q)_B$ are the fluxes of s and q at z_B (Fig. 9). The turbulent eddy fluxes jump to zero across the infinitely thin transition layer, the layer between z_B and z_B+.

To derive equations for the time change of z_B we consider the heat and moisture budgets in the infinitely thin transition layer shown in Fig. 9. The total vertical mass flux M_B beneath the clouds, at level z_B, is given by

$$M_B\equiv M_c(z_B)=\int_0^{\lambda_{\max}}\mathfrak{M}_B(\lambda)d\lambda. \tag{110}$$

The subsidence between the clouds at the top of the mixed layer is given by $M_B-\rho_B\bar{w}_B$. The mass flux into the mixed layer, the depth of which may be changing with time, is given by $\rho_B(Dz_B/Dt-\bar{w}_B)+M_B$. The downward fluxes of s and q through the top of the transition layer, at $z=z_B+$, are

$$(s_M+\Delta s)\left\{\rho_B\left(\frac{Dz_B}{Dt}-\bar{w}_B\right)+M_B\right\}, \tag{111}$$

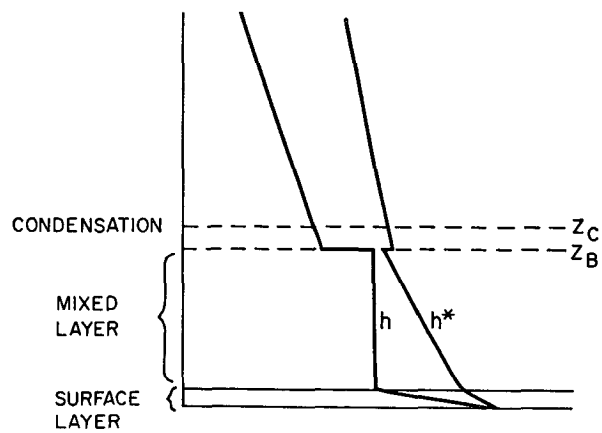

FIG. 10. A schematic diagram of typical vertical profiles of h and h^* near the mixed layer. h is constant with height in the mixed layer, and h^* decreases rapidly with height in the mixed layer since the temperature lapse rate is dry adiabatic.

$$(q_M+\Delta q)\left\{\rho_B\left(\frac{Dz_B}{Dt}-\bar{w}_B\right)+M_B\right\}. \tag{112}$$

The downward fluxes of s and q through the bottom of the transition layer, at z_B, are

$$s_M\left[\rho_B\left(\frac{Dz_B}{Dt}-\bar{w}_B\right)+M_B\right]-(F_s)_B, \tag{113}$$

$$q_M\left[\rho_B\left(\frac{Dz_B}{Dt}-\bar{w}_B\right)+M_B\right]-(F_q)_B, \tag{114}$$

where we have defined

$$\frac{D}{Dt}=\frac{\partial}{\partial t}+\bar{\mathbf{v}}_B\cdot\nabla. \tag{115}$$

The continuity of heat and moisture fluxes across z_B yields

$$\rho_B\frac{Dz_B}{Dt}=-(M_B-\rho_B\bar{w}_B)-\frac{1}{\Delta s}(F_s)_B, \tag{116}$$

$$\rho_B\frac{Dz_B}{Dt}=-(M_B-\rho_B\bar{w}_B)-\frac{1}{\Delta q}(F_q)_B. \tag{117}$$

Here, we have ignored the possible discontinuity of the radiation flux at z_B. This effect is of critical importance when the upper part of the mixed layer is saturated and has a layer of stratus cloud (see Lilly, 1968), but not with our unsaturated mixed layer. Consistency of (116) and (117) requires

$$(F_q)_B=\frac{\Delta q}{\Delta s}(F_s)_B. \tag{118}$$

A relation between the fluxes of virtual s at the bottom and top of the mixed layer can be derived from the turbulent energy balance, following Lilly (1968). We let

$$(F_{sv})_B=-k(F_{sv})_0. \tag{119}$$

The flux of virtual s is given by

$$F_{sv}=F_s+c_pT\delta F_q, \tag{120}$$

where T is a reference temperature and $\delta=0.608$; k takes a value between 0 and 1. Lilly (1968) discussed the extreme cases $k=0$ and $k=1$, which he called the minimum and maximum entrainment cases. The minimum entrainment case corresponds to total frictional dissipation of turbulent kinetic energy, while the maximum entrainment case corresponds to zero frictional dissipation of turbulent kinetic energy. Deardorff *et al.* (1969) suggested $k\approx0.10$ from laboratory experiments on non-steady penetrative convection in a water tank. Betts (1973a) suggested $k\approx0.25$.

Eqs. (118), (119) and (120) can be combined to give

$$(F_s)_B=-\frac{k\Delta s}{\Delta s_v}(F_{sv})_0, \tag{121}$$

$$(F_q)_B=-\frac{k\Delta q}{\Delta s_v}(F_{sv})_0, \tag{122}$$

where

$$\Delta s_v=\Delta s+c_pT\delta\Delta q. \tag{123}$$

Positive Δs_v is required for dry convective stability. Eqs. (121) and (122) show that with an upward surface flux of virtual s, there is a downward flux of s and an upward flux of q at z_B. This is shown schematically in Fig. 9.

Eqs. (105), (106), (116), (121) and (122) combine to give

$$\rho_M\frac{\partial s_M}{\partial t}=-(\rho\bar{\mathbf{v}})_M\cdot\nabla s_M+\frac{1}{z_B}\left[(F_s)_0+k\frac{\Delta s}{\Delta s_v}(F_{sv})_0\right]+(Q_R)_M, \tag{124}$$

$$\rho_M\frac{\partial q_M}{\partial t}=-(\rho\bar{\mathbf{v}})_M\cdot\nabla q_M+\frac{1}{z_B}\left[(F_q)_0+k\frac{\Delta q}{\Delta s_v}(F_{sv})_0\right], \tag{125}$$

$$\rho_B\frac{Dz_B}{Dt}=-(M_B-\rho_B\bar{w}_B)+\frac{k}{\Delta s_v}(F_{sv})_0. \tag{126}$$

Eqs. (124) and (125) give

$$\rho_M\frac{\partial h_M}{\partial t}=-(\rho\bar{\mathbf{v}})_M\cdot\nabla h_M+\frac{1}{z_B}\left[(F_h)_0+k\frac{\Delta h}{\Delta s_v}(F_{sv})_0\right]+(Q_R)_M, \tag{127}$$

where $(F_h)_0$ is the surface flux of h.

In (124)–(127), Δs_v appears as a denominator. When Δs_v is small, a direct estimate of Δs_v may be inaccurate. Following Deardorff *et al.* (1969) and Betts (1973a), we derive the following approximate alternative expression for Δs_v, which may be used when Δs_v is small (see Appendix A):

$$\Delta s_v\approx\frac{k}{1+k}z_B\left(\frac{\partial\delta_v}{\partial z}\right)_{z=z_{B+}}, \quad \text{for small } \Delta s_v. \tag{128}$$

Eq. (126) reflects the fact that what determines the mass inflow into the mixed layer is the entrainment due to turbulent eddies, which depends on the turbulent eddy flux of virtual s at the surface. Without the entrainment, the top of the mixed layer is simply pushed down by the subsidence, $M_B-\rho_B\bar{w}_B$.

Without cumulus clouds ($M_B=0$), the depth of the mixed layer increases with time when $\rho_B\bar{w}_B+k(F_{sv})_0/\Delta s_v>0$. With cumulus clouds, however, the cumulus-induced subsidence between the clouds counteracts the

deepening of the mixed layer. When the cumulus ensemble is very active, the cumulus-induced subsidence may even make the mixed layer shallower. However, the mixed layer cannot become too shallow, because the shallower it becomes the smaller is the fraction of air which enters the cloud from the mixed layer, and the greater is the fraction of air which enters the cloud from the environment above the mixed layer; and that environmental air has not been reached by the turbulent upward transport of moisture. A shallow mixed layer is therefore not favorable for maintaining an intensely active cumulus ensemble. In this sense, the variable depth of the mixed layer is part of the mechanism which controls the total mass flux into the clouds from the mixed layer. Betts (1973a) obtained M_B from (126) and (128), for a given $\bar{w}_B$ and $(F_{sv})_0$, assuming $z_B=z_C$. We do not assume $z_B=z_C$, but instead let z_B vary with time, in order to let the depth of the mixed layer be one of the controls on the intensity of the cumulus convection. A more quantitative formulation of this mechanism is given later in this paper.

In this section, we have shown that z_B, s_M and q_M, and therefore h_M, can be determined prognostically. However, there remains the question of whether it is adequate to replace $s_c(z_B,\lambda)$, $q_c(z_B,\lambda)$ and $h_c(z_B,\lambda)$ by the characteristic values s_M, q_M and h_M in the mixed layer. This depends on whether the cumulus clouds have their roots in the thermodynamical variables within the mixed layer. It has been reported that cloud roots are not observed in the mixed layer for trade-wind cumuli (Bunker *et al.*, 1949; Malkus, 1952). In general, evaporation from falling precipitation would make $s_c(z_B,\lambda)$ lower than s_M and $q_c(z_B,\lambda)$ higher than q_M, but would leave h_M unmodified. The liquid water mixing ratio $\hat{l}(z)$ does depend on $q_c(z_B,\lambda)$, but it depends even more on how we parameterize the rainfall $r(z,\lambda)$. Apparently, some perturbations of the mixed layer are necessary for triggering the onset of a cloud within an otherwise uniform environment. But even then, the perturbation could be on z_B, rather than on s_M or q_M (see Malkus, 1963). In this paper, we postulate that the primary role of the mixed layer is to supply moisture and static energy to the cumulus clouds and, therefore, we let

$$s_c(z_B,\lambda)=s_M, \tag{129}$$

$$q_c(z_B,\lambda)=q_M, \tag{130}$$

$$h_c(z_B,\lambda)=h_M. \tag{131}$$

6. The cloud work function

Our final problem is to find the mass flux distribution function, $\mathfrak{M}_B(\lambda)$. The real conceptual difficulty in parameterizing cumulus convection starts from this point. We must determine how the large-scale processes control the spectral distribution of clouds, in terms of the mass flux distribution function, if they indeed do so at all. This is the essence of the parameterization problem.

For the special case in which the mass flux distribution function has a sharp maximum around a certain λ, the entrainment relationship (94) will give the predominant size of the clouds. In this particular case, therefore, finding $\mathfrak{M}_B(\lambda)$ will also solve the problem of the cumulus size. However, as Simpson (1971) stated, "Although cumulus size appears to be at least roughly proportional to the horizontal convergence in the synoptic regime, what really determines the scale of convection remains one of the critical unsolved problems in meteorology."

The solution for $\mathfrak{M}_B(\lambda)$ may be even more difficult than just the determination of the predominant cloud size; instead, we must determine the entire spectrum of the clouds. But, on the other hand, in a parameterization theory it is necessary to find only the statistical properties of the cumulus ensemble, under given large-scale conditions, and not the properties of each individual cloud at a given place and time. Also, with the approximations that are used in this parameterization theory, we need to obtain only the mass flux distribution function, $\mathfrak{M}_B(\lambda)$, and not necessarily the population distribution in λ space. These two are generally not equivalent.

As preparation for an attempt to solve the problem, which will be made in the next section, we now look into the generation of the kinetic energy of cumulus convection.

The time change of the kinetic energy of each subensemble can be written as

$$\frac{d\mathfrak{K}(\lambda)}{dt}=A(\lambda)\mathfrak{M}_B(\lambda)-\mathfrak{D}(\lambda), \tag{132}$$

where $\mathfrak{K}(\lambda)d\lambda$ and $\mathfrak{D}(\lambda)d\lambda$ are, respectively, the kinetic energy and its dissipation rate due to the circulations associated with all the clouds which have fractional entrainment rates between λ and $\lambda+d\lambda$. The first term on the right in (132) is the rate of generation of kinetic energy due to work done by buoyancy forces, i.e., $A(\lambda)$ is the kinetic energy generation per unit $\mathfrak{M}_B(\lambda)d\lambda$. It is important to note that (132) holds for two- or three-dimensional cumulus convection, in which mass continuity is satisfied in a vertically bounded domain and which allows kinetic energy conversion between vertical and horizontal velocity components. However, mechanical interactions of the cumulus convection with the vertical shear of the horizontal velocity of the environment and with other types of clouds are neglected.

We call $A(\lambda)$ the "cloud work function." Because $A(\lambda)$ is the kinetic energy generation per unit mass flux, it is a measure of the efficiency of the kinetic energy generation. It is given by

$$A(\lambda)=\int_{z_B}^{z_D(\lambda)}\frac{g}{c_p\bar{T}(z)}\eta(z,\lambda)[s_{vc}(z,\lambda)-\bar{s}_v(z)]dz, \tag{133}$$

where $\eta(z,\lambda)$ is the previously defined normalized mass flux and $g[s_{vc}(z,\lambda)-\bar{s}_v(z)]/(c_p\bar{T})$ the buoyancy force. Therefore, $A(\lambda)$ is an integral measure of the buoyancy force with the weighting function $\eta(z,\lambda)$.

It is important to note that the buoyancy force for a given λ is a property of the environment, including the subcloud mixed layer. For simplicity, let us temporarily neglect the difference between static energy and virtual static energy. Eqs. (97), (98) and (131) give

$$\eta(z,\lambda)[s_c(z,\lambda)-\bar{s}(z)]$$
$$=\frac{1}{1+\gamma(z)}\left[h_M+\lambda\int_{z_B}^{z}\eta(z',\lambda)\bar{h}(z')dz'-\eta(z,\lambda)\bar{h}^*(z)\right],$$
$$\text{for}\quad z_C(\lambda)\leqslant z\leqslant z_D(\lambda), \quad (134)$$

and Eqs. (98)′ and (129) give

$$\eta(z,\lambda)[s_c(z,\lambda)-\bar{s}(z)]$$
$$=s_M+\lambda\int_{z_B}^{z}\eta(z',\lambda)\bar{s}(z')dz'-\eta(z,\lambda)\bar{s}(z),$$
$$\text{for}\quad z_B\leqslant z\leqslant z_C(\lambda). \quad (135)$$

From (134) and (135), we see that the buoyancy force [and, therefore, the detrainment level $z_D(\lambda)$] for each λ is completely determined by the thermodynamical vertical structure of the environment.[7] Then, the cloud work function $A(\lambda)$, which is given by (133), is also determined for each λ by the thermodynamical vertical structure of the environment. Moreover, the cloud work function is the only property of the environment which can influence the kinetic energy generation of type λ clouds.

In the special case of $z_C(\lambda)=z_B+$, substitution of (134) into (133) gives

$$A(\lambda)=\int_{z_B}^{z_D(\lambda)}\rho(z)\beta(z)$$
$$\times\left[h_M+\lambda\int_{z_B}^{z}\eta(z',\lambda)\bar{h}(z')dz'-\eta(z,\lambda)\bar{h}^*(z)\right]dz, \quad (136)$$

where[8]

$$\rho(z)\beta(z)\equiv\frac{g}{c_p\bar{T}(z)[1+\gamma(z)]}. \quad (137)$$

Using the identity

$$\eta(z,\lambda)\bar{h}^*(z)=\bar{h}^*(z_B+)+\int_{z_{B+}}^{z}\frac{\partial}{\partial z'}[\eta(z',\lambda)\bar{h}^*(z')]dz' \quad (138)$$

and Eq. (95) in (136), we obtain

$$A(\lambda)=\int_{z_B}^{z_D(\lambda)}\rho(z)\beta(z)\left[h_M-\bar{h}^*(z_B+)+\int_{z_{B+}}^{z}\eta(z',\lambda)\right.$$
$$\left.\times\left\{\lambda[\bar{h}(z')-\bar{h}^*(z')]-\frac{\partial\bar{h}^*(z')}{\partial z'}\right\}dz'\right]dz, \quad (139)$$

where $\rho(z)\beta(z)[h_M-\bar{h}^*(z_B+)]$ is the buoyancy at cloud base; $-\partial\bar{h}^*(z)/\partial z$ is positive when the lapse rate exceeds the moist adiabatic lapse rate. When there is no buoyancy at cloud base $[h_M=\bar{h}^*(z_B+)]$, and the environment is saturated $(\bar{h}=\bar{h}^*)$, (139) is simply an integral measure of the conditional instability, $-\partial\bar{h}^*/\partial z$. When the environment is not saturated, the contribution to $A(\lambda)$ by $\bar{h}-\bar{h}^*$ [i.e., $L(\bar{q}-\bar{q}^*)$] is always negative and opposes the positive contribution by the conditional instability. To have positive $A(\lambda)$, which is necessary for kinetic energy generation, the environment must not only be conditionally unstable, but it must also be moist enough to give a sufficiently small $|\bar{h}-\bar{h}^*|$. This effect becomes increasingly important as λ increases. Non-entraining clouds, for which $\lambda=0$, are not influenced by the environmental humidity above the cloud base. $A(\lambda)>0$ can therefore be considered as a generalized criterion for moist convective instability. Because of entrainment, the criterion depends on cloud type. The condition $A(\lambda)=0$ for all λ gives a neutral environment.

Logically, $A(\lambda)>0$ is not a sufficient condition for kinetic energy generation. Actual kinetic energy generation depends also on $\mathfrak{M}_B(\lambda)$, for the kinetic energy generation is zero when $\mathfrak{M}_B(\lambda)=0$, regardless of the value $A(\lambda)$. However, we have seen that $A(\lambda)$ is also a measure of moist convective instability. We therefore expect the development of cumulus clouds, and consequently the increase of $\mathfrak{M}_B(\lambda)$ whenever $A(\lambda)>0$, provided that there is a triggering mechanism to get the cumulus convection started.

In order for $\mathfrak{M}_B(\lambda)$ to reach a significant size, $A(\lambda)$ must remain positive for a sufficient length of time. This motivates us to look into the time change of the cloud work function $A(\lambda)$.

Because the cloud work function depends only on the vertical distributions of the static energy and the water vapor mixing ratio in the environment, including the subcloud mixed layer, the prognostic equations (74), (75), (124), (125) and (126), which govern the time derivatives of $\bar{s}(z)$, $\bar{q}(z)$, s_M, q_M and z_B, respectively, are sufficient to give the time derivative of the cloud work function. These prognostic equations involve terms of two types: "cloud terms," which depend on the mass flux distribution function either through the total vertical mass flux, $M_c(z)$ (or M_B), or through the total detrainment $D(z)$; and "large-scale terms," such as large-scale advection, surface eddy fluxes, and radia-

[7] This conclusion also holds when the virtual static energy is used.

[8] Later we redefine $\beta(z)$ to include an effect of the difference between static energy and virtual static energy.

tional heating terms, which do not depend on the mass flux distribution function. Then the time derivative of the cloud work function can be expressed as a summation of cloud terms and large-scale terms. We may write

$$\frac{dA(\lambda)}{dt}=\left[\frac{dA(\lambda)}{dt}\right]_C+\left[\frac{dA(\lambda)}{dt}\right]_{LS}, \qquad (140)$$

where the subscripts C and LS denote, respectively, the cloud terms and the large-scale terms.

We call the large-scale terms the large-scale forcing $F(\lambda)$. Positive $F(\lambda)$ means a positive rate of increase of the cloud work function (destabilization), for cloud type λ, by large-scale processes. The cloud terms linearly depend on $M_c(z)$ and $D(z)$. $M_c(z)$ is a linear integral transform of $\mathfrak{M}_B(\lambda)$ [see (77) and (80)]. $D(z)$ also linearly depends on $\mathfrak{M}_B(\lambda)$ [see (79) and (80)]. Thus, the cloud terms linearly depend on $\mathfrak{M}_B(\lambda)$. Because the whole spectrum of cloud types participates in determining $M_c(z)$ and $D(z)$, we may write the cloud terms in the form

$$\left[\frac{dA(\lambda)}{dt}\right]_C=\int_0^{\lambda_{\max}}K(\lambda,\lambda')\mathfrak{M}_B(\lambda')d\lambda'. \qquad (141)$$

Typically, the kernel $K(\lambda,\lambda')$ is negative. Then $K(\lambda,\lambda')\times\mathfrak{M}_B(\lambda')d\lambda'$ is the rate of decrease (stabilization) of the cloud work function for type λ clouds through the modification of the environment by type λ' clouds. Eq. (140) is now rewritten as

$$\frac{dA(\lambda)}{dt}=\int_0^{\lambda_{\max}}K(\lambda,\lambda')\mathfrak{M}_B(\lambda')d\lambda'+F(\lambda). \qquad (142)$$

The actual forms of $F(\lambda)$ and $K(\lambda,\lambda')$ as well as their derivations are given in Appendix B.

The large-scale forcing can be divided into two parts:

$$F(\lambda)=F_C(\lambda)+F_M(\lambda), \qquad (143)$$

where $F_C(\lambda)$ originates from the large-scale terms in Eqs. (74) and (75) [we call $F_C(\lambda)$ the "cloud layer forcing"]; and $F_M(\lambda)$ originates from the large-scale terms in Eqs. (124), (125) and (126) [we call $F_M(\lambda)$ the "mixed layer forcing"].

The most dominant effect in the cloud layer forcing seems to be the increase of the cloud work function due to the cooling of the environment above the mixed layer by large-scale processes, typically by adiabatic cooling due to large-scale upward motion. The mixed layer forcing includes the increase of the cloud work function through the deepening effects on the depth of the mixed layer by large-scale upward velocity at the top of the mixed layer, and by the upward flux of virtual static energy at the earth's surface. An examination of the relative importance of $F_C(\lambda)$ and $F_M(\lambda)$, for actual observed situations, will be presented in Part II of this paper (Schubert and Arakawa, 1974).

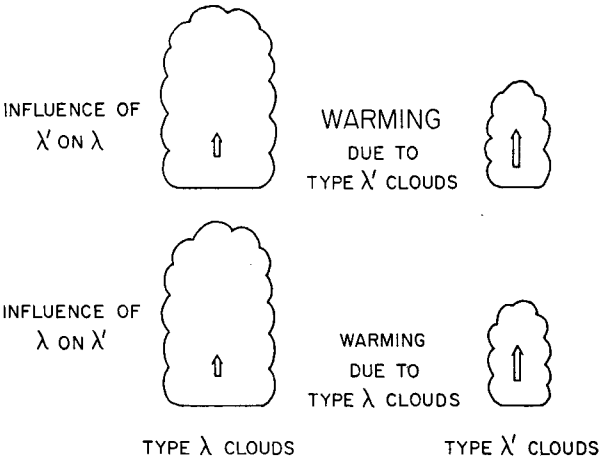

FIG. 11. A schematic diagram of the mutual influence of a subensemble pair through the first part of the vertical mass flux kernel. The arrows inside the clouds show the normalized vertical mass fluxes $\eta(z,\lambda)$ and $\eta(z,\lambda')$; $\eta(z,\lambda')>\eta(z,\lambda)$ because $\lambda'>\lambda$. In the upper part of the figure, the warming of the environment due to type λ' clouds is shown, and in the lower part of the figure, the warming of the environment due to type λ clouds is shown. Note that (warming due to type λ clouds)$\times\eta(z,\lambda')=$(warming due to type λ' clouds)$\times\eta(z,\lambda)$ holds for $z_B<z<z_D(\lambda')$, which is the entire depth of the mutual influence.

The kernel can be divided into three parts:

$$K(\lambda,\lambda')=K_V(\lambda,\lambda')+K_D(\lambda,\lambda')+K_M(\lambda), \qquad (144)$$

where $K_V(\lambda,\lambda')$, $K_D(\lambda,\lambda')$ and $K_M(\lambda)$ originate, respectively, from $M_c(z)$ in (74) and (75), $D(z)$ in (74) and (75), and M_B in (126). We call $K_V(\lambda,\lambda')$ the "vertical mass flux kernel," $K_D(\lambda,\lambda')$ the "detrainment kernel," and $K_M(\lambda)$ the "mixed layer kernel."

The most dominant effect in the vertical mass flux kernel (and also in the entire kernel) is typically the decrease of the cloud work function, for type λ clouds, through adiabatic warming of the environment due to the subsidence induced by type λ' clouds. If the other effects in $K_V(\lambda,\lambda')$ are neglected, $K_V(\lambda,\lambda')$ is symmetric with respect to λ and λ'. This symmetry of $K_V(\lambda,\lambda')$

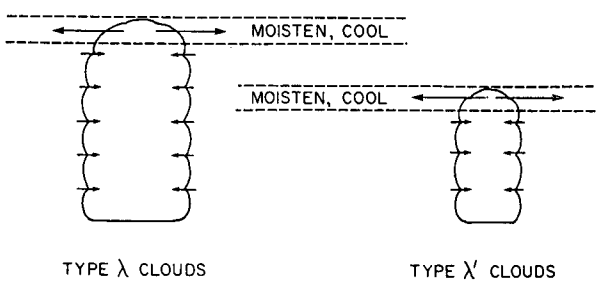

FIG. 12. A schematic diagram of the influence of type λ' clouds on type λ clouds through the detrainment process. The detraining air is saturated and contains liquid water. The detrainment moistens and evaporatively cools the environment. Type λ clouds have no influence on type λ' clouds but type λ' clouds have a cooperative influence on type λ clouds.

means that the amount of decrease of $A(\lambda)$ by type λ' clouds, per unit $\mathfrak{M}_B(\lambda')d\lambda'$ (through the mechanism described above), is equal to the decrease of $A(\lambda')$ by type λ clouds, per unit $\mathfrak{M}_B(\lambda)d\lambda$. This situation is illustrated in Fig. 11.

The detrainment kernel is zero for $\lambda'<\lambda$, and nearly always positive for $\lambda'>\lambda$. This means that shallower clouds increase the cloud work function of deeper clouds through cooling of the environment (by the evaporation of detrained liquid water) and through moistening of the environment (by the evaporation and the detrainment of the saturated air from clouds). This situation is illustrated in Fig. 12.

The role of a varying z_B in controlling the intensity of the cumulus convection was discussed in Section 5. This role is included in the mixed layer kernel.

7. The quasi-equilibrium assumption

The purpose of cumulus parameterization is to relate the statistical properties of a cumulus cloud ensemble to the large-scale variables, and thereby to obtain a closed system of prognostic equations for the large-scale variables. We have already shown that such a closed system will be obtained if we can determine the mass flux distribution function, $\mathfrak{M}_B(\lambda)$, which is the sub-ensemble vertical mass flux at the top of the mixed layer. However, there is no *a priori* reason to believe that this is always possible.

One might take the view that the mass flux distribution is determined entirely by subcloud layer processes. This point of view is supported by one-dimensional cumulus cloud models, in which the horizontal velocity components and induced pressure gradients are neglected. With the exception of precipitation effects, such one-dimensional cloud models do not allow dynamical interaction between the upper and lower parts of the cloud. An initial cloud base condition determines the solution only along a characteristic line in the z-t plane. While such a model can predict the height and some other properties of the cloud top reasonably well, the prediction of the properties of the cloud air which is not near the cloud top is doubtful, unless proper cloud base conditions are given as a continuous time sequence of "initial" conditions. Because a one-dimensional cloud model does not allow the dynamical process above cloud base to control the cloud base conditions, a continuous sequence of "initial" conditions can be specified independently, as long as an updraft is given near the cloud base. Therefore, only the local subcloud layer processes remain as a possible mechanism for determining the cloud base conditions.

The situation is different in models which have more than one dimension. An impulse is still needed, if the initial condition is otherwise horizontally uniform, but only for the first cloud to get started. After the initial time, the cloud base conditions for the first cloud and for all subsequent clouds cannot be specified, for they are a part of the solution of the entire system of equations, which includes the dynamics of both the cloud and subcloud layers.

Small turbulent perturbations in the mixed layer below the clear environment are not likely to trigger new clouds, if the top of the mixed layer is sufficiently below the condensation level. Thus, the formation of new clouds between existing clouds usually requires stronger impulses, possibly stimulated by the downdrafts associated with neighboring clouds. Otherwise, a new cloud (or a new active part of a cloud) is likely to form in the wake of a preceding cloud (or a preceding active part of a cloud), because the solenoidal field associated with the preceding cloud (or the preceding active part of the cloud) produces a circulation in a vertical plane. The cloud work function, $A(\lambda)$, defined in the last section, is an integral measure of this solenoidal field.

It was pointed out in Section 4 that the sub-ensemble mass flux is the population times the mass flux of a single cloud averaged in time over its entire life. At level z_B, we have

$$\mathfrak{M}_B(\lambda)d\lambda=\frac{\mathfrak{N}(\lambda)d\lambda}{\tau(\lambda)}\mathrm{M}_B(\lambda). \tag{145}$$

Here $\mathfrak{N}(\lambda)d\lambda$ is the population of the sub-ensemble, $\tau(\lambda)$ the lifetime, and $\mathrm{M}_B(\lambda)$ the vertical mass flux, at level z_B, of a *single cloud integrated over its entire lifetime*. Because all clouds which exist at time t must have formed during the time interval $[t-\tau(\lambda), t]$, $\mathfrak{N}(\lambda)d\lambda/\tau(\lambda)$ is the rate of cloud formation. This corresponds to the "dispatcher function" of Ooyama (1971). $\mathrm{M}_B(\lambda)$ is the total mass which passes level z_B through the entire life of a single cloud. If we represent each cloud by a spherical bubble, as Ooyama (1971) did, the total mass becomes the mass of the bubble, which depends only on its radius. Because the radius is related to the fractional rate of entrainment λ, through an entrainment relation similar to (94), the total mass $\mathrm{M}_B(\lambda)$ becomes a prescribed function of λ, which remains the same regardless of the large-scale conditions. Then the mass flux distribution function $\mathfrak{M}_B(\lambda)$ for different large-scale conditions is controlled only through different "dispatcher functions." This agrees with Ooyama's conclusion. However, if we do not assume sphericity, or any other prescribed geometry which relates the vertical dimension to the horizontal size, the functional form for $\mathrm{M}_B(\lambda)$ is unknown. $\mathrm{M}_B(\lambda)$ is a gross measure of the activity of a single cloud of type λ, and it is highly probable that large-scale conditions control the mass flux distribution function by giving different functional forms to $\mathrm{M}_B(\lambda)$.

The numerical simulation of a cloud with the "one-and-a-half" dimensional model of Ogura and Takahashi (1971) clearly shows that the time-integrated mass flux near cloud base is highly sensitive to the rate of conversion of cloud droplets to rain drops (see Fig. 7 of their paper). When the conversion rate is sufficiently

small, the cloud attains a steady state[9] [i.e., $M_B(\lambda)$ is infinitely large], while with larger conversion rates the cloud undergoes a life cycle [$M_B(\lambda)$ is finite]. According to Ogura and Takahashi's interpretation, this difference is due to the drag force by raindrops in the middle portion of the cloud where the buoyancy force is acting. This does not directly show that $M_B(\lambda)$ is sensitive to the large-scale conditions, but it does indicate that $M_B(\lambda)$ is sensitive to work done by forces *in* the cloud, i.e., the kinetic energy generation or destruction.

Recently, rapid progress toward the realistic simulation of cumulus clouds has been made with two-dimensional models, notably by Árnason *et al.* (1968, 1969), Árnason and Greenfield (1972), Murray (1970), Murray and Koenig (1972), Orville (1968), Orville and Sloan (1970), Takeda (1971), and Wilhelmson and Ogura (1972). But those studies have been limited to the formation and decay of a single cloud. There has been no numerical simulation of a cumulus cloud ensemble, analogous to the numerical simulation of the general circulation of the atmosphere.

Due to our lack of theoretical understanding and empirical knowledge, we do not attempt in this paper to determine $\mathfrak{N}(\lambda)$, $\tau(\lambda)$ and $M_B(\lambda)$ separately, although that should be an eventual goal of statistical cumulus dynamics. In the rest of this section, we will show that this separation is not necessary to determine the mass flux distribution function, $\mathfrak{M}_B(\lambda)$, if a cumulus ensemble is in quasi-equilibrium with the large-scale forcing. We will also show observational verification of the quasi-equilibrium assumption.

However, in order to understand the quasi-equilibrium, some physical insight into the transient phase is necessary. Suppose that we perform a numerical simulation experiment with an initial condition in which there is no cumulus convection and no large-scale forcing, but in which the vertical distributions of temperature and moisture give a positive cloud work function $A(\lambda)$ for a certain range of λ. Cumulus clouds will then develop, provided that there is a triggering mechanism, and the mass flux distribution function will increase with time. Then, modification of the environment by the cumulus clouds, through the cloud terms in (74), (75) and (126), will begin. Typically, the modification will warm and dry the environment above the mixed layer and decrease the depth of the mixed layer. Such modification of the environment will produce a smaller buoyancy force in the clouds and, therefore, a smaller cloud work function. This decrease of the cloud work function (stabilization) is through the cloud terms in (140). If the large-scale forcing remains negligible in time,[10] this stabilization and kinetic energy dissipation will eventually make the cumulus cloud activity die out. The final state will be a neutral state [i.e., $A(\lambda)=0$ for the entire range of λ] with no cumulus clouds. We call the time needed for this adjustment to a neutral state, "the adjustment time."

However, if there is a counteracting increase of the cloud work function (destabilization) by large-scale forcing, the cumulus activity will be maintained. As an idealization, let us ignore any time change of the large-scale forcing. Then the adjustment will not be toward a neutral state, with no cumulus clouds, but will be toward an equilibrium state determined by the large-scale forcing. This equilibrium is characterized by $dA(\lambda)/dt=0$, i.e., by the exact balance of the cloud and large-scale terms in (142). At least when the large-scale forcing is weak, the equations which govern the adjustment process are approximately linear and, therefore, the time needed to reach the equilibrium state will be about the same as the adjustment time.

Usually the large-scale forcing is changing in time and, therefore, the cumulus ensemble will not reach an exact equilibrium. The properties of the cumulus ensemble will then depend on the past history of the large-scale forcing, but this dependency should be significant only within the time scale of the adjustment time. When the time scale of the large-scale forcing, τ_{LS}, is sufficiently longer than the adjustment time, τ_{ADJ}, the past history, within the time scale of the adjustment time, can be represented by the current large-scale forcing. This means that the cumulus ensemble follows a sequence of quasi-equilibria with the current large-scale forcing. We assume that this is the case for the cumulus ensembles we wish to parameterize. We call this assumption "the quasi-equilibrium assumption." It is also an assumption on parameterizability, if by parameterization we mean a relation between the properties of the cumulus ensemble and the large-scale variables at the same instant. Unless a cumulus ensemble is in quasi-equilibrium with the large-scale processes, we cannot uniquely relate the statistical properties of the ensemble to the large-scale variables.

The problem we are considering is a problem with two time scales: τ_{ADJ}, the adjustment time scale, and τ_{LS}, the time scale of the large-scale processes. Quasi-equilibrium exists when $\tau_{ADJ} \ll \tau_{LS}$.[11] When the adjustment process is filtered out, we obtain a sequence of quasi-equilibria. In such a sequence, the large-scale forcing and the cumulus ensemble vary in time in a coupled way and, therefore, the time scale of the statistical properties of the ensemble is equal to the time scale of the large-scale processes, τ_{LS}.

In a sequence of quasi-equilibria, $dA(\lambda)/dt$ is generally not zero. But following an argument similar to that given by Arakawa (1969), we can see that for such a sequence $dA(\lambda)/dt$ in (140) is negligibly small. The role of the cloud terms in (140) is to restore

[9] The time change of the environment is neglected in their model.

[10] This will be true if conditional instability of the second kind does not exist.

[11] This situation is somewhat analogous to quasi-geostrophic balance, which occurs when $1/f \ll L/V$, where $1/f$ is the time scale of geostrophic adjustment and L/V the advective time scale.

$A(\lambda)$ toward zero with time scale τ_{ADJ}. Then the order of magnitude of the cloud term is given by

$$\left|\left[\frac{dA(\lambda)}{dt}\right]_C\right| \sim \frac{1}{\tau_{ADJ}} A(\lambda). \tag{146}$$

On the other hand, the order of magnitude of the actual $dA(\lambda)/dt$, in a sequence of quasi-equilibria, is given by

$$\left|\frac{dA(\lambda)}{dt}\right| \lesssim \frac{1}{\tau_{LS}} A(\lambda). \tag{147}$$

Combining (146) and (147), we obtain

$$\left|\frac{dA(\lambda)}{dt}\right| \lesssim \frac{\tau_{ADJ}}{\tau_{LS}} \left|\left[\frac{dA(\lambda)}{dt}\right]_C\right|. \tag{148}$$

Therefore, when $\tau_{ADJ}/\tau_{LS} \ll 1$,

$$\left|\frac{dA(\lambda)}{dt}\right| \ll \left|\left[\frac{dA(\lambda)}{dt}\right]_C\right|, \tag{149}$$

and the left-hand side of (140) [and therefore of (142)] can be neglected. Then we obtain

$$\int_0^{\lambda_{\max}} K(\lambda,\lambda')\mathfrak{M}_B(\lambda')d\lambda' + F(\lambda) = 0 \tag{150}$$

as an approximate equation which governs the mass flux distribution function $\mathfrak{M}_B(\lambda)$.

Since $\tau_{ADJ}/\tau_{LS} \ll 1$ is a sufficient condition to justify (150), the inequality sign in (147) is not necessary. This means $A(\lambda)$ is not necessarily constant in time over the time scale τ_{LS}, even in an approximate sense. A more general interpretation of our approximation is that $A(\lambda)$ itself is small, because (146), (149) and (140) give

$$A(\lambda) \sim \tau_{ADJ}\left|\left[\frac{dA(\lambda)}{dt}\right]_C\right| \sim \tau_{ADJ}\left|\left[\frac{dA(\lambda)}{dt}\right]_{LS}\right|. \tag{151}$$

Eq. (151) means that $A(\lambda)$ is of the order of the increase of the cloud work function, due to the large-scale processes alone, over the short period of τ_{ADJ}. Because $A(\lambda)=0$ means a neutral state, a sequence of quasi-equilibria can now be interpreted as a sequence of quasi-neutral states.

Because we are not able to determine τ_{ADJ} theoretically, we estimate its order of magnitude empirically. From (133), the order of magnitude of $A(\lambda)$ is given by $A \sim gH_c(T_c-\bar{T})/\bar{T}$, where H_c is the depth of the cloud. Observations show that the excess temperature of clouds, $T_c-\bar{T}$, is of the order of a few degrees, so that

$$A \sim (10^{-1}\ \text{m sec}^{-2})H_c. \tag{152}$$

We now estimate $[dA(\lambda)/dt]_C$ from the dominant term in the kernel K_V, which represents adiabatic warming of the environment due to cumulus-induced subsidence. We obtain $(dA(\lambda)/dt)_C \sim gH_c(M_c/\rho)(\partial\bar{s}/\partial z)/c_p\bar{T} \sim N^2\sigma_c w_c H_c$, where $N^2 = g(\partial\bar{s}/\partial z)/c_p\bar{T} = (g\partial\ \ln\bar{\theta}/\partial z) \sim 10^{-4}$ sec^{-2}. Because $\sigma_c \lesssim 10^{-1}$ and $w_c \lesssim 10$ m sec^{-1}, we obtain $\sigma_c w_c \lesssim 1$ m sec^{-1}. If we use $\sigma_c w_c \sim (10^{-1}$–$1$ m sec$^{-1})$,

$$\left(\frac{dA(\lambda)}{dt}\right)_C \sim (10^{-4}\text{–}10^{-5}\text{m sec}^{-3})H_c. \tag{153}$$

From (152), (153) and (146), we obtain

$$\tau_{ADJ} \sim (10^3\text{–}10^4)\ \text{sec}. \tag{154}$$

Typically, $\tau_{LS} \gtrsim 10^5$ sec. Then τ_{ADJ} is at least one to two orders of magnitude smaller than τ_{LS}.

A more precise observational verification of the quasi-equilibrium assumption has been made with the Marshall Islands data, provided by Yanai *et al.* (1973). Because the cloud work function is a property of the thermodynamical structure of the environment (and therefore of the large-scale field), we can calculate the cloud work function from radiosonde observations. From a time series of such data, we can calculate $dA(\lambda)/dt$. The large-scale forcing $F(\lambda)$ can also be calculated from observations if wind observations at a network of stations are available. Fig. 13 gives examples of such calculations. We can see, from the figure, that the observed $dA(\lambda)/dt$ is much smaller than $F(\lambda)$.[12] This indicates that (150) is a good approximation.

It is important to note that quasi-equilibrium does not mean quasi-steady temperature and moisture fields on the time scale τ_{LS}. A sequence of quasi-equilibria is usually a sequence of different quasi-neutral states. In such a sequence, time changes of the temperature and moisture fields are not completely independent, because the quasi-neutral condition $A(\lambda) \approx 0$ must be maintained, if type λ clouds exist. Fig. 14 shows an example of such a sequence. The calculations are based on observations at Eniwetok in the Marshall Islands, which is located in the ITCZ. In the figure, $I_1(\lambda)$ and $I_2(\lambda)$ are defined by

$$I_1(\lambda) = \int_{z_B}^{z_D(\lambda)} \rho(z)\beta(z) \times\left[h_M + \lambda\int_{z_B}^{z}\eta(z',\lambda)\bar{h}(z')dz'\right]dz, \tag{155}$$

$$I_2(\lambda) = \int_{z_B}^{z_D(\lambda)} \rho(z)\beta(z)\eta(z,\lambda)\bar{h}^*(z)dz, \tag{156}$$

and the approximate cloud work function (136) is given by

$$A(\lambda) = I_1(\lambda) - I_2(\lambda). \tag{157}$$

[12] Due to the difficulty in determining $F_M(\lambda)$ from conventional data, this term was not calculated. A rough estimate, however, shows that $F_M(\lambda)$ is considerably smaller than $F_C(\lambda)$, with this set of data.

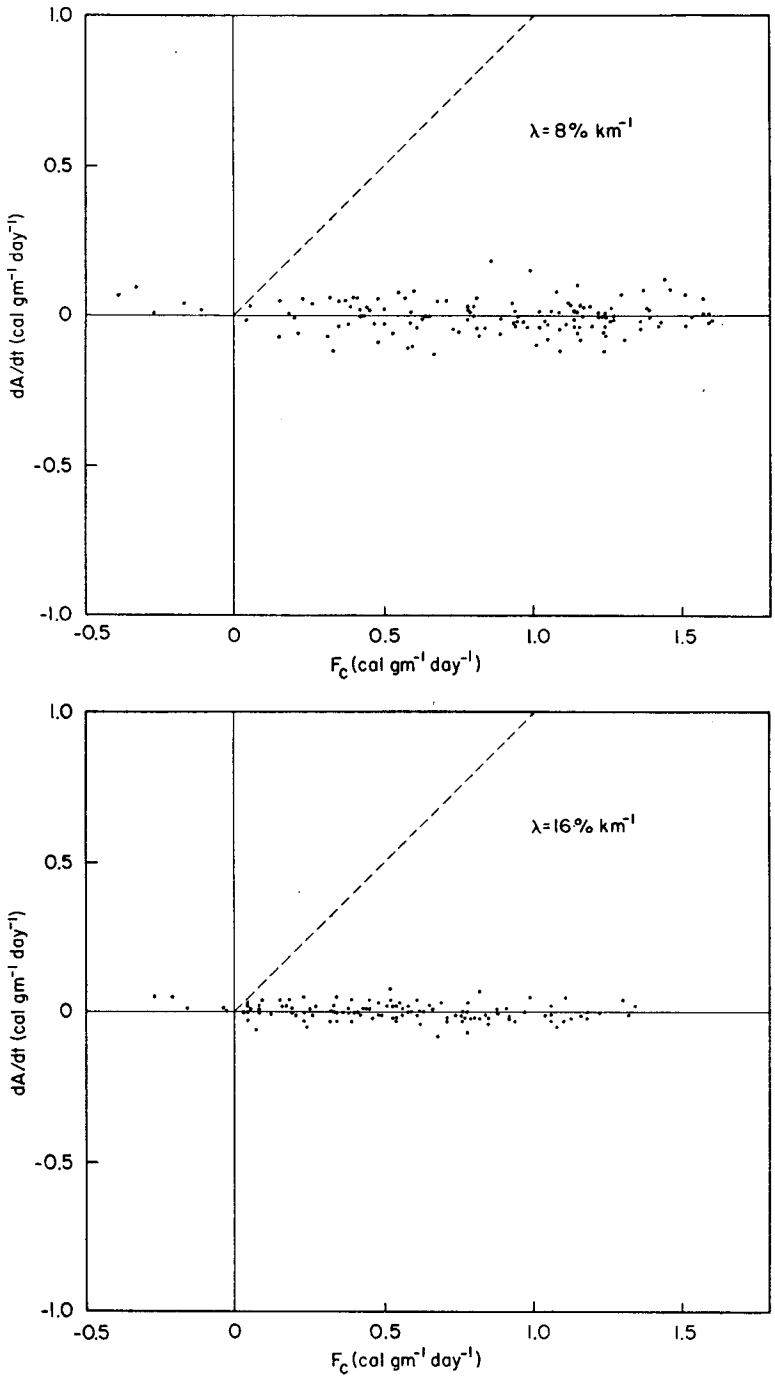

FIG. 13. An observational verification of the quasi-equilibrium assumption for cloud types $\lambda=8\%\,\mathrm{km}^{-1}$ and $\lambda=16\%\,\mathrm{km}^{-1}$, with the Marshall Islands data provided by Yanai *et al.* (1973). The abscissa is the cloud layer forcing $F_C(\lambda)$ and the ordinate is the observed time derivative of the cloud work function, $dA(\lambda)/dt$. The top of the mixed layer and cloud base are both assumed to be at 950 mb. Zero buoyancy at cloud base is also assumed. The dashed line is the line along which $dA(\lambda)/dt = F_C(\lambda)$.

As an example, $I_1(\lambda)$ and $I_2(\lambda)$ for $\lambda=8\%$ km^{-1} is shown. Throughout the period shown in the figure, $A(\lambda)$ is positive (so that cumulus clouds of that type may exist) but it is only slightly positive. Relatively large time changes of $I_1(\lambda)$ and $I_2(\lambda)$ compared to their difference, $A(\lambda)$, indicates that although this is not a steady state, it is a sequence of quasi-neutral states. Because $I_1(\lambda)$ depends on the vertical distributions of

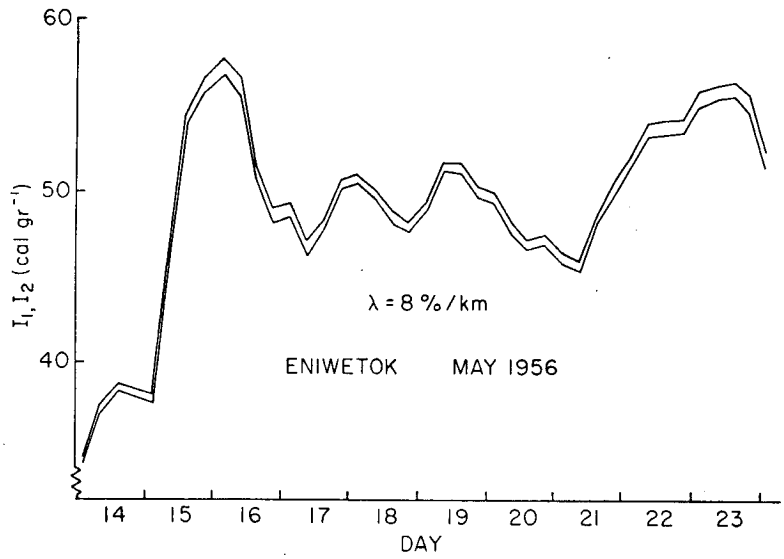

FIG. 14. A time sequence of $I_1(\lambda)$ and $I_2(\lambda)$ for cloud type $\lambda = 8\%$ km^{-1} at Eniwetok in the Marshall Islands.

both temperature and moisture, while $I_2(\lambda)$ depends on the vertical distribution of temperature only, the small difference between the two, throughout the period, indicates the presence of a constraint on the time changes of the temperature and moisture fields, which is the constraint of quasi-neutrality.

We now have a closed parameterization of cumulus convection. Eq. (150) is a Fredholm integral equation of the first kind for the unknown $\mathfrak{M}_B(\lambda)$. By solving the integral equation, we can obtain the mass flux distribution function which is needed for the prediction equations (74), (75) and (126).

The integral equation (150) must hold for each cloud type which exists, i.e., it must hold for each cloud type for which $\mathfrak{M}_B(\lambda)>0$. When $A(\lambda)$ is zero or negative, we assume that the corresponding cloud type λ does not exist $[\mathfrak{M}_B(\lambda)=0]$. Even when $A(\lambda)$ is positive (but only slightly positive), cloud type λ may still not exist because the net increase of $A(\lambda)$ by the large-scale forcing plus the forcing due to other cloud types through the kernel $K(\lambda,\lambda')$ for $\lambda'\neq\lambda$, may be negative. Because a cloud type λ cannot increase its own $A(\lambda)$, in that situation $dA(\lambda)/dt<0$, and we can therefore assume that $\mathfrak{M}_B(\lambda)$ is zero. A formal solution of (150), which neglects $dA(\lambda)/dt$, gives a negative $\mathfrak{M}_B(\lambda)$ for that cloud type. In other words, $\mathfrak{M}_B(\lambda)$ must satisfy

$$\left.\begin{aligned} &\mathfrak{M}_B(\lambda)>0 \quad \text{and} \quad \int_0^{\lambda_{\max}} K(\lambda,\lambda')\mathfrak{M}_B(\lambda')d\lambda' \\ &\qquad\qquad +F(\lambda)=0 \\ &\text{or} \\ &\mathfrak{M}_B(\lambda)=0 \quad \text{and} \quad \int_0^{\lambda_{\max}} K(\lambda,\lambda')\mathfrak{M}_B(\lambda')d\lambda' \\ &\qquad\qquad +F(\lambda)<0 \end{aligned}\right\} \tag{158}$$

for each λ.

The inequalities in (158) are conditions on the unknown $\mathfrak{M}_B(\lambda)$. This poses an additional mathematical difficulty, in addition to the usual difficulties associated with the numerical solution of Fredholm integral equations of the first kind. But a simple iterative method which overcomes these difficulties has been developed by Schubert and Arakawa (1974). This method was successful when applied to solutions of (158) for actual observed situations.

8. Summary and conclusions

A theory of the mutual interaction of a cumulus cloud ensemble with the slowly changing large-scale environment, including the subcloud mixed layer, is presented.

Section 2 considers the budgets of mass, static energy and water vapor for the environment above the mixed layer. These budget equations describe the way in which an existing cumulus ensemble modifies the thermodynamical structure of the environment. With the assumption that the total fractional area covered by cumulus clouds is much smaller than unity, prediction equations for the large-scale thermodynamical fields are derived.

Section 3 considers the budgets of mass, static energy, water vapor and liquid water of an individual cloud, for both its entrainment and detrainment layers. The detrainment layer is assumed to be a thin layer near the level of vanishing buoyancy. This assumption simplifies the prediction equations obtained in Section 2. It is concluded that the modification of the large-scale thermodynamical fields by a cumulus ensemble depends on the total vertical mass flux in the clouds, which determines the cumulus-induced subsidence in the environment, on the total mass detrainment from

the clouds into the environment, and on the mixing ratio of liquid water at the levels of vanishing buoyancy.

Section 4 gives a spectral representation of the cumulus ensemble. The cumulus ensemble is divided into sub-ensembles according to the fractional entrainment rate. It is shown that the sub-ensemble budget equations determine the thermodynamical properties of each sub-ensemble, at all levels, if the conditions at the top of the subcloud mixed layer are known.

Section 5 considers the budgets of mass, static energy and water vapor for the subcloud mixed layer. It is assumed that the turbulent eddy fluxes vanish discontinuously at the top of the mixed layer and, therefore, that the transition layer between the mixed layer and the cloud environment above is infinitesimally thin. From the corresponding budgets for this transition layer, a prediction equation is derived for the depth of the mixed layer. The equation for the depth of the mixed layer, the budget equations for the mixed layer, the sub-ensemble budget equations (of Section 4), and the prediction equations for the large-scale fields (of Section 3), together describe the way in which the mixed layer, the cumulus ensemble, and the environment above the mixed layer mutually interact. The problem of cumulus parameterization is thus reduced to the determination of the mass flux distribution function, which is the sub-ensemble vertical mass flux at the top of the mixed layer.

Section 6 introduces the cloud work function. It is a property of the thermodynamical structure of the large-scale environment and is a generalized measure of the moist convective instability which depends on cloud type. For the cumulus activity to be maintained in time, the cloud work function must remain positive. By considering the time derivative of the cloud work function, destabilization or stabilization by the large-scale processes (large-scale forcing) and by cumulus convective processes (adjustment) are identified.

Section 7 introduces the quasi-equilibrium assumption and gives its observational verification. This quasi-equilibrium, which is the closure condition for parameterizability, occurs when the time scale of the large-scale forcing is much longer than the time scale of the ajustsment. A sequence of quasi-equilibria can be interpreted as a sequence of different quasi-neutral states, so that the time changes of the temperature and moisture fields are constrained, as long as the cumulus activity continues. To satisfy this constraint, the mass flux distribution function, which couples the time changes of the temperature and the moisture fields, cannot be arbitrary. It is shown that the mass flux distribution function, under quasi-equilibrium, must satisfy a Fredholm integral equation of the first kind. This is the principal conclusion of Part I of this paper.

Adjustment toward a quasi-equilibrium, which can be interpreted as a quasi-neutral state, is crucial in this parameterization theory. It is important to note, however, that the actual value of the adjustment time does not appear in the integral equation (150). Only the existence of an adjustment mechanism which has a time scale much smaller than the time scale of the large-scale processes was assumed. In the first approximation, the actual value of the adjustment time does not matter in describing the quasi-equilibrium because the adjustment is practically instantaneous (Arakawa, 1969).

The non-homogeneous term of the integral equation, which is the large-scale forcing $F(\lambda)$, describes the way in which large-scale processes control a cumulus ensemble. Although the actual form of $F(\lambda)$, given in Appendix B, may appear complicated, it is not necessary to calculate the individual terms of $F(\lambda)$ when using this theory in numerical simulation models. From the numerical modeling point of view, we need only know $[dA(\lambda)/dt]_{LS}\Delta t$, the net change of the cloud work function in the finite time interval Δt due to large-scale processes alone. If we assume that $A(\lambda)$ remains practically zero for a sequence of quasi-equilibria, the temporary non-zero $A(\lambda)$, which results from the finite time step prediction of the temperature and moisture fields by the large-scale processes alone, is regarded as $[dA(\lambda)/dt]_{LS}\Delta t$. After solving (158) for $\mathfrak{M}_B(\lambda)\Delta t$ with this $[dA(\lambda)/dt]_{LS}\Delta t$ as the large-scale forcing, we can calculate the additional time changes of the temperature and moisture fields by the cloud terms in (74) and (75). These changes bring the temporary non-zero value of $A(\lambda)$ back to zero. This calculational procedure has a formal similarity to the moist convective adjustment method of Manabe *et al.* (1965). In their method, the large-scale forcing is implicit while the adjustment is explicit.

On the other hand, for the theoretical understanding of the large-scale forcing mechanism, we need an explicit form for $F(\lambda)$. With the explicit form of $F(\lambda)$, our parameterization can be viewed as a generalization of earlier parameterizations by Charney and Eliassen (1964), Ooyama (1964) and Kuo (1965), in which large-scale forcing was explicit while adjustment was implicit. In their parameterizations the large-scale forcing was expressed in terms of either large-scale frictional convergence in the planetary boundary layer or large-scale moisture convergence in the entire vertical column. These effects can be identified in our large-scale forcing, $F(\lambda)$, which has a more general form. In addition to a generalization of the predominant effects of the large-scale vertical velocity, $F(\lambda)$ includes the effects of large-scale horizontal advection, surface sensible and latent heat fluxes and radiational heating (or cooling).

Several applications of this theory have already been made. The authors themselves have developed an iterative numerical method for solving the integral equation. This method has been applied to calculations of the mass flux distribution function, using observations from a large-scale network of stations in the ITCZ region. The results, as well as the method, will be presented in Part II of this paper (Schubert and

Arakawa, 1974). In addition, a discretized version of the parameterization has been developed and incorporated into the UCLA general circulation model by Chao *et al.* (1974).

A part of this theory (the equations presented in Sections 2, 3 and 4) has been used for diagnostic determinations of the mass flux distribution function, with times series of large-scale observations independently by Ogura and Cho (1973) and Nitta (1974).

The theory, in a simplified form, has also been used for studies of CISK by Israeli and Sarachik (1973) and by Arakawa and Chao (1973). Using a two-cloud type version of the theory, in a three-level quasi-geostrophic model for large-scale motion, Arakawa and Chao found that tropical cyclones have a maximum growth rate when the size is several hundred kilometers.

Acknowledgments. We wish to thank Prof. Michio Yanai for valuable discussion on this problem and for providing the observational data which was used in this paper. Thanks are also due to Prof. Yale Mintz for his encouragement and for his careful review of the manuscript. The senior author would also like to thank Prof. Jule Charney for his interest in this work and for stimulating discussion, especially during a visit to MIT in the summer of 1972.

The research reported here was supported by the National Science Foundation under Grant NSF GA 34306, and by the National Aeronautics and Space Administration, Institute for Space Studies, Goddard Space Flight Center, under Grant NGR 05-007-328.

APPENDIX A

An Approximate Expression for Δs_v

From the definition of Δs_v, we can write

$$\frac{D}{Dt}\Delta s_v=\frac{D}{Dt}[\bar{s}_v(z_B+)-s_{vM}], \tag{A1}$$

where D/Dt is defined by (115) and $s_{vM}=s_M+c_pT\delta q_M$. Eq. (A1) can be rewritten as

$$\frac{D}{Dt}\Delta s_v=\left(\frac{\partial\bar{s}_v}{\partial z}\right)_{z=z_B+}\frac{Dz_B}{Dt}+\left(\frac{D\bar{s}_v}{Dt}\right)_{z=z_B+}-\frac{Ds_{vM}}{Dt}. \tag{A2}$$

Using the large-scale budget equation for $\bar{s}_v$, and assuming there is no detrainment from the clouds at z_B+, (A2) becomes

$$\rho_B\frac{D}{Dt}\Delta s_v=\left[\rho_B\left(\frac{Dz_B}{Dt}-\bar{w}_B\right)+M_B\right]\left(\frac{\partial\bar{s}_v}{\partial z}\right)_{z=z_B+}+\bar{Q}_R(z_B+)-\rho_B\frac{Ds_{vM}}{Dt}. \tag{A3}$$

When $D\Delta s_v/Dt$, $(\bar{\mathbf{v}}_B-(\rho\mathbf{v})_M/\rho_M)\cdot\nabla s_{vM}$ and $\bar{Q}_R(z_B+)-(Q_R)_M$ are small, (A3) can be written

$$\rho_B\frac{Dz_B}{Dt}=-(M_B-\rho_B\bar{w}_B)+\frac{1+k}{z_B\left(\dfrac{\partial\bar{s}_v}{\partial z}\right)_{z=z_B+}}(F_{sv})_0. \tag{A4}$$

Here we have used (120), (123)–(125), and the definition of s_{vM}. Comparing (A4) with (126), we obtain an approximate expression for Δs_v given by (128).

APPENDIX B

Derivation of $K(\lambda,\lambda')$ and $F(\lambda)$

The actual forms of the kernel $K(\lambda,\lambda')$ and the large-scale forcing $F(\lambda)$ are derived by taking the time derivative of (133). We define

$$\rho(z)\alpha(z)\equiv\frac{g}{c_p\bar{T}(z)}, \tag{B1}$$

$$\rho(z)\beta(z)\equiv\frac{g}{c_p\bar{T}(z)}\left[\frac{1+\gamma(z)\epsilon(z)\delta}{1+\gamma(z)}\right], \tag{B2}$$

where $\epsilon(z)\equiv c_p\bar{T}(z)/L$ and $\delta=0.608$. Using

$$\frac{g}{c_p\bar{T}(z)}[s_{vc}(z,\lambda)-\bar{s}_v(z)]=\rho(z)\beta(z)[h_c(z,\lambda)-\bar{h}^*(z)]+g\delta[\bar{q}^*(z)-\bar{q}(z)]-gl(z,\lambda) \tag{B3}$$

for the buoyancy force when $z_C(\lambda)\leqslant z\leqslant z_D(\lambda)$, the time derivative of (133) can be written

$$\frac{\partial A(\lambda)}{\partial t}=\int_{z_B}^{z_C(\lambda)}\eta(z,\lambda)\frac{\partial}{\partial t}\Big\{\rho(z)\alpha(z)[s_{vc}(z,\lambda)-\bar{s}_v(z)]\Big\}dz+\int_{z_C(\lambda)}^{z_D(\lambda)}\eta(z,\lambda)\frac{\partial}{\partial t}\Big\{\rho(z)\beta(z)[h_c(z,\lambda)-\bar{h}^*(z)]+g\delta[\bar{q}^*(z)-\bar{q}(z)]-gl(z,\lambda)\Big\}dz-\frac{\partial z_B}{\partial t}\Big\{-\rho_B\alpha(z_B)\Delta s_v+\lambda A(\lambda)\Big\}. \tag{B4}$$

We shall ignore time changes of $\rho(z)\alpha(z)$ and $\rho(z)\beta(z)$. The last term in (B4) comes from the time change of z_B in $\eta(z,\lambda)$ and from the time change of the lower limit of integration in (133), with the aid of (129) and (130). A term involving the time change of $z_D(\lambda)$ does not appear in (B4) since we are assuming that there is no buoyancy at $z_D(\lambda)$.

In order to reduce (B4) to the form given by (140), we must first express the time derivatives of the cloud quantities $s_{vc}(z,\lambda)$, $h_c(z,\lambda)$ and $l(z,\lambda)$ in terms of time derivatives of the large-scale fields. The time derivative of $h_c(z,\lambda)$ can be found from (97) and (131). It is given

by

$$\eta(z,\lambda)\frac{\partial h_c(z,\lambda)}{\partial t}=\frac{\partial h_M}{\partial t}+\lambda\int_{z_B}^{z}\eta(z',\lambda)\frac{\partial\bar{h}(z')}{\partial t}dz'-\frac{\partial z_B}{\partial t}\lambda\Delta h, \quad \text{(B5)}$$

for, $z_B\leqslant z\leqslant z_D(\lambda)$. Since both $s_c(z,\lambda)$ and $q_c(z,\lambda)$ satisfy equations similar to (97) between z_B and $z_C(\lambda)$, the time derivative of $s_{vc}(z,\lambda)$ is given by

$$\eta(z,\lambda)\frac{\partial s_{vc}(z,\lambda)}{\partial t}=\frac{\partial s_{vM}}{\partial t}+\lambda\int_{z_B}^{z}\eta(z',\lambda)\frac{\partial\bar{s}_v(z')}{\partial t}dz'-\frac{\partial z_B}{\partial t}\lambda\Delta s_v, \quad \text{(B6)}$$

for $z_B\leqslant z\leqslant z_C(\lambda)$.

If $r(z,\lambda)$ is parameterized by $C_0\,l(z,\lambda)$, where C_0 is a constant, the solution of (85) is

$$\eta(z,\lambda)l(z,\lambda)=\int_{z_B}^{z}e^{-C_0(z-z')}\left\{-\frac{\partial}{\partial z'}[\eta(z',\lambda)q_c(z',\lambda)]+\lambda\eta(z',\lambda)\bar{q}(z')\right\}dz'. \quad \text{(B7)}$$

The lower limit of integration in (B7) can be either z_B or $z_C(\lambda)$ since the integrand vanishes between these two levels. As long as $z_C(\lambda)$ lies above z_B, the time derivative of $l(z,\lambda)$ is given by

$$\eta(z,\lambda)\frac{\partial l(z,\lambda)}{\partial t}=\int_{z_B}^{z}e^{-C_0(z-z')}\eta(z',\lambda)\times\frac{\partial}{\partial t}\left\{-\frac{\partial q_c(z',\lambda)}{\partial z'}-\lambda[q_c(z',\lambda)-\bar{q}(z')]\right\}dz', \quad \text{(B8)}$$

for $z_B\leqslant z\leqslant z_D(\lambda)$.

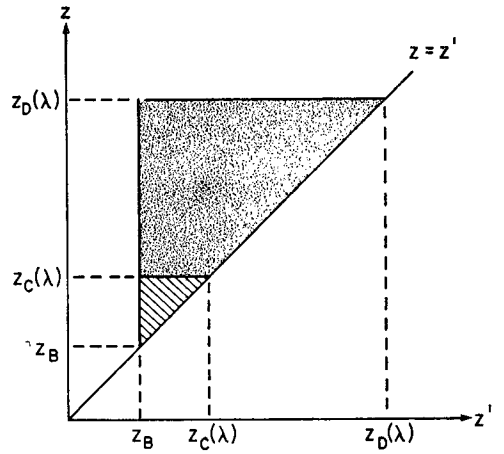

FIG. 15. A diagram of the z'-z domain, showing the areas of integration which appear in Eq. (B11).

From the definition of virtual static energy and $L\partial\bar{q}^*(z)/\partial t=\gamma(z)\partial\bar{s}(z)/\partial t$, we obtain

$$-\rho(z)\beta(z)\frac{\partial\bar{h}^*(z)}{\partial t}+g\delta\frac{\partial}{\partial t}[\bar{q}^*(z)-\bar{q}(z)]=-\rho(z)\alpha(z)\frac{\partial\bar{s}_v(z)}{\partial t}. \quad \text{(B9)}$$

From (90) we obtain

$$L\frac{\partial}{\partial t}\left\{\frac{\partial q_c(z,\lambda)}{\partial z}+\lambda[q_c(z,\lambda)-\bar{q}(z)]\right\}=\frac{\lambda}{1+\gamma(z)}\frac{\partial}{\partial t}[\bar{h}^*(z)-\bar{h}(z)]+\frac{\partial h_c(z,\lambda)}{\partial t}\frac{\partial}{\partial z}\left[\frac{\gamma(z)}{1+\gamma(z)}\right], \quad \text{(B10)}$$

for $z_C(\lambda)\leqslant z\leqslant z_D(\lambda)$. Using (B5), (B6), (B8), (B9) and (B10), (B4) can be written

$$\begin{aligned}\frac{\partial A(\lambda)}{\partial t}=&\frac{\partial s_{vM}}{\partial t}\int_{z_B}^{z_C(\lambda)}\alpha(z)\rho(z)dz+\frac{\partial h_M}{\partial t}\int_{z_C(\lambda)}^{z_D(\lambda)}\left\{\beta(z)\rho(z)+\frac{g}{L}\int_{z_B}^{z}e^{-C_0(z-z')}\frac{\partial}{\partial z'}\left(\frac{\gamma(z')}{1+\gamma(z')}\right)dz'\right\}dz\\
&-\frac{\partial z_B}{\partial t}\left\{\Delta s_v\left[-\rho_B\alpha(z_B)+\lambda\int_{z_B}^{z_C(\lambda)}\alpha(z)\rho(z)dz\right]\right.\\
&\left.+\Delta h\,\lambda\int_{z_C(\lambda)}^{z_D(\lambda)}\left[\beta(z)\rho(z)+\frac{g}{L}\int_{z_B}^{z}e^{-C_0(z-z')}\frac{\partial}{\partial z'}\left(\frac{\gamma(z')}{1+\gamma(z')}\right)dz'\right]dz+\lambda A(\lambda)\right\}\\
&+\int_{z_B}^{z_C(\lambda)}\alpha(z)\rho(z)\left\{\lambda\int_{z_B}^{z}\eta(z',\lambda)\frac{\partial\bar{s}_v(z')}{\partial t}dz'-\eta(z,\lambda)\frac{\partial\bar{s}_v(z)}{\partial t}\right\}dz+\int_{z_C(\lambda)}^{z_D(\lambda)}\left\{\beta(z)\rho(z)\left[\lambda\int_{z_B}^{z}\eta(z',\lambda)\frac{\partial\bar{h}(z')}{\partial t}dz'\right]\right.\\
&\left.-\alpha(z)\rho(z)\eta(z,\lambda)\frac{\partial\bar{s}_v(z)}{\partial t}+\frac{g}{L}\lambda\int_{z_B}^{z}e^{-C_0(z-z')}\left[\eta(z',\lambda)\left(\frac{1}{1+\gamma(z')}\right)\frac{\partial}{\partial t}[\bar{h}^*(z')-\bar{h}(z')]\right.\right.\\
&\left.\left.+\frac{\partial}{\partial z'}\left(\frac{\gamma(z')}{1+\gamma(z')}\right)\int_{z_B}^{z'}\eta(z'',\lambda)\frac{\partial\bar{h}(z'')}{\partial t}dz''\right]dz'\right\}dz. \quad \text{(B11)}\end{aligned}$$

In (B11) there appear five double integrals and one triple integral. The first two double integrals are identical and are integrations over the stippled area in Fig. 15. Reversing the order of integration, the first and second double integrals can be written

$$\frac{g}{L}\int_{z_C(\lambda)}^{z_D(\lambda)}\left\{\int_{z'}^{z_D(\lambda)} e^{-C_0(z-z')}\,dz\right\}\frac{\partial}{\partial z'}\left(\frac{\gamma(z')}{1+\gamma(z')}\right)dz'+\frac{g}{L}\int_{z_B}^{z_C(\lambda)}\left\{\int_{z_C(\lambda)}^{z_D(\lambda)} e^{-C_0(z-z')}\,dz\right\}\frac{\partial}{\partial z'}\left(\frac{\gamma(z')}{1+\gamma(z')}\right)dz'. \quad \text{(B12)}$$

The third double integral is over the hatched triangular area in Fig. 15. Reversing the order of integration, the third double integral can be written

$$\int_{z_B}^{z_C(\lambda)}\left\{\int_{z'}^{z_C(\lambda)}\alpha(z)\rho(z)dz\right\}\lambda\eta(z',\lambda)\frac{\partial\bar{s}_v(z')}{\partial t}dz'. \quad \text{(B13)}$$

Similarly, the fourth double integral can be written as

$$\int_{z_C(\lambda)}^{z_D(\lambda)}\left\{\int_{z'}^{z_D(\lambda)}\beta(z)\rho(z)dz\right\}\lambda\eta(z',\lambda)\frac{\partial\bar{h}(z')}{\partial t}dz'+\int_{z_B}^{z_C(\lambda)}\left\{\int_{z_C(\lambda)}^{z_D(\lambda)}\beta(z)\rho(z)dz\right\}\lambda\eta(z',\lambda)\frac{\partial\bar{h}(z')}{\partial t}dz', \quad \text{(B14)}$$

and the fifth double integral as

$$\frac{g}{L}\int_{z_C(\lambda)}^{z_D(\lambda)}\left\{\int_{z'}^{z_D(\lambda)} e^{-C_0(z-z')}dz\right\}\eta(z',\lambda)\left(\frac{\lambda}{1+\gamma(z')}\right)\frac{\partial}{\partial t}[\bar{h}^*(z')-\bar{h}(z')]dz'$$
$$+\frac{g}{L}\int_{z_B}^{z_C(\lambda)}\left\{\int_{z_C(\lambda)}^{z_D(\lambda)} e^{-C_0(z-z')}dz\right\}\eta(z',\lambda)\left(\frac{\lambda}{1+\gamma(z')}\right)\frac{\partial}{\partial t}[\bar{h}^*(z')-\bar{h}(z')]dz'. \quad \text{(B15)}$$

The triple integral in (B11) can be written

$$\int_{z_C(\lambda)}^{z_D(\lambda)}\left\{\int_{z''}^{z_D(\lambda)}\left[\frac{g}{L}\int_{z'}^{z_D(\lambda)} e^{-C_0(z-z')}dz\right]\frac{\partial}{\partial z'}\left(\frac{\gamma(z')}{1+\gamma(z')}\right)dz'\right\}\lambda\eta(z'',\lambda)\frac{\partial\bar{h}(z'')}{\partial t}dz''$$
$$+\int_{z_B}^{z_D(\lambda)}\left\{\int_{z_C(\lambda)}^{z_D(\lambda)}\left[\frac{g}{L}\int_{z'}^{z_D(\lambda)} e^{-C_0(z-z')}dz\right]\frac{\partial}{\partial z'}\left(\frac{\gamma(z')}{1+\gamma(z')}\right)dz'\right\}\lambda\eta(z'',\lambda)\frac{\partial\bar{h}(z'')}{\partial t}dz''$$
$$+\int_{z_B}^{z_C(\lambda)}\left\{\int_{z''}^{z_C(\lambda)}\left[\frac{g}{L}\int_{z_C(\lambda)}^{z_D(\lambda)} e^{-C_0(z-z')}dz\right]\frac{\partial}{\partial z'}\left(\frac{\gamma(z')}{1+\gamma(z')}\right)dz'\right\}\lambda\eta(z'',\lambda)\frac{\partial\bar{h}(z'')}{\partial t}dz''. \quad \text{(B16)}$$

Using (B12)–(B16) and the definitions

$$\rho(z)a(z,\lambda)\equiv\begin{cases}0, & z_C(\lambda)\leqslant z\leqslant z_D(\lambda)\\ \displaystyle\int_z^{z_C(\lambda)}\alpha(z')\rho(z')dz', & z_B\leqslant z\leqslant z_C(\lambda),\end{cases} \quad \text{(B17)}$$

$$\rho(z)b(z,\lambda)\equiv\begin{cases}\displaystyle\int_z^{z_D(\lambda)}\beta(z')\rho(z')dz', & z_C(\lambda)\leqslant z\leqslant z_D(\lambda)\\ \displaystyle\int_{z_C(\lambda)}^{z_D(\lambda)}\beta(z')\rho(z')dz', & z_B\leqslant z\leqslant z_C(\lambda),\end{cases} \quad \text{(B18)}$$

$$\rho(z)c(z,\lambda)\equiv\int_z^{z_D(\lambda)}d(z',\lambda)\frac{\partial}{\partial z'}\left(\frac{\gamma(z')}{1+\gamma(z')}\right)\rho(z')dz', \qquad z_B\leqslant z\leqslant z_D(\lambda), \quad \text{(B19)}$$

$$\rho(z)d(z,\lambda)\equiv\begin{cases}\displaystyle\frac{g}{L}\int_z^{z_D(\lambda)} e^{-C_0(z'-z)}dz', & z_C(\lambda)\leqslant z\leqslant z_D(\lambda)\\ \displaystyle\frac{g}{L}\int_{z_C(\lambda)}^{z_D(\lambda)} e^{-C_0(z'-z)}dz', & z_B\leqslant z\leqslant z_C(\lambda),\end{cases} \quad \text{(B20)}$$

(B11) can be written

$$\frac{\partial A(\lambda)}{\partial t}=a(z_B,\lambda)\rho_B\frac{\partial s_{vM}}{\partial t}+[b(z_B,\lambda)+c(z_B,\lambda)]\rho_B\frac{\partial h_M}{\partial t}$$
$$-\rho_B\frac{\partial z_B}{\partial t}\left\{[-\alpha(z_B)+\lambda a(z_B,\lambda)]\Delta s_v+\lambda[b(z_B,\lambda)+c(z_B,\lambda)]\Delta h+\lambda\frac{A(\lambda)}{\rho_B}\right\}+\int_{z_B}^{z_D(\lambda)}\eta(z,\lambda)\left\{[-\alpha(z)+\lambda a(z,\lambda)]\frac{\partial\bar{s}_v(z)}{\partial t}\right.$$
$$\left.+\lambda[b(z,\lambda)+c(z,\lambda)-(1+\gamma(z))^{-1}d(z,\lambda)]\frac{\partial\bar{h}(z)}{\partial t}+\lambda d(z,\lambda)\frac{\partial\bar{s}(z)}{\partial t}\right\}\rho(z)dz. \quad \text{(B21)}$$

The first three terms on the right-hand side of (B21) involve time changes of the mixed layer variables, s_{vM}, h_M and z_B. The last term in (B21) involves time changes of the temperature and moisture fields above the top of the mixed layer. The time change of s_{vM} is derived from (124) and (125) and can be written

$$\rho_M\frac{\partial s_{vM}}{\partial t}=-(\rho\bar{\mathbf{v}})_M\cdot\nabla s_{vM}+\frac{1+k}{z_B}(F_{sv})_0. \quad \text{(B22)}$$

The time change of h_M is given by (127), while the time change of z_B is given by (126), which can also be written as

$$\rho_B\frac{\partial z_B}{\partial t}=-M_B+\rho_B\left(\frac{\partial z_B}{\partial t}\right)_{LS}. \quad \text{(B23)}$$

The time change of $\bar{s}$ is given by (74) while the time changes of $\bar{s}_v$ and $\bar{h}$ can be derived from (74) and (75). Thus,

$$\rho\frac{\partial\bar{s}}{\partial t}=D(\hat{s}-\bar{s}-L\hat{l})+M_c\frac{\partial\bar{s}}{\partial z}+\rho\left(\frac{\partial\bar{s}}{\partial t}\right)_{LS}, \quad \text{(B24)}$$

$$\rho\frac{\partial\bar{s}_v}{\partial t}=-DL[1-(1+\delta)\epsilon]\hat{l}+M_c\frac{\partial\bar{s}_v}{\partial z}+\rho\left(\frac{\partial\bar{s}_v}{\partial t}\right)_{LS}, \quad \text{(B25)}$$

$$\rho\frac{\partial\bar{h}}{\partial t}=D[\hat{h}^*-\bar{h}^*+L(\bar{q}^*-\bar{q})]+M_c\frac{\partial\bar{h}}{\partial z}+\rho\left(\frac{\partial\bar{h}}{\partial t}\right)_{LS}. \quad \text{(B26)}$$

In (B23) through (B26) we have defined

$$\rho_B\left(\frac{\partial z_B}{\partial t}\right)_{LS}\equiv-\rho_B\bar{\mathbf{v}}_B\cdot\nabla z_B+\rho_B\bar{w}_B+\frac{k}{\Delta s_v}(F_{sv})_0, \quad \text{(B27)}$$

$$\rho\left(\frac{\partial\bar{s}}{\partial t}\right)_{LS}\equiv-\rho\bar{w}\frac{\partial\bar{s}}{\partial z}-\rho\bar{\mathbf{v}}\cdot\nabla\bar{s}+\bar{Q}_R, \quad \text{(B28)}$$

$$\rho\left(\frac{\partial\bar{s}_v}{\partial t}\right)_{LS}\equiv-\rho\bar{w}\frac{\partial\bar{s}_v}{\partial z}-\rho\bar{\mathbf{v}}\cdot\nabla\bar{s}_v+\bar{Q}_R, \quad \text{(B29)}$$

$$\rho\left(\frac{\partial\bar{h}}{\partial t}\right)_{LS}\equiv-\rho\bar{w}\frac{\partial h}{\partial z}-\rho\bar{\mathbf{v}}\cdot\nabla\bar{h}+\bar{Q}_R. \quad \text{(B30)}$$

Eqs. (B23) through (B26) involve terms of two types: terms due to cumulus convection and terms due to large-scale processes. Radiation and surface sensible and latent heat fluxes are included in the definition of large-scale processes. The mixed layer equations (B22) and (127) contain only large-scale terms. The terms due to cumulus convection in (B24)–(B26) can be further divided into detrainment terms and vertical mass flux terms. Let us now substitute (B23)–(B26) into the right-hand side of (B21) and divide the result into terms of three types: detrainment terms, vertical mass flux terms, and large-scale terms. This yields

$$\frac{\partial A(\lambda)}{\partial t}=\int_{z_B}^{z_D(\lambda)}\eta(z,\lambda)\left\{[1-(1+\delta)\epsilon(z)][\alpha(z)-\lambda a(z,\lambda)]L\hat{l}(z)\right.$$
$$\left.+\lambda[b(z,\lambda)+c(z,\lambda)-(1+\gamma(z))^{-1}d(z,\lambda)][\hat{h}^*(z)-\bar{h}^*(z)+L(\bar{q}^*(z)-\bar{q}(z))]+\lambda d(z,\lambda)[\hat{s}(z)-\bar{s}(z)-L\hat{l}(z)]\right\}D(z)dz$$
$$+\int_{z_B}^{z_D(\lambda)}\eta(z,\lambda)\left\{[-\alpha(z)+\lambda a(z,\lambda)]\frac{\partial\bar{s}_v}{\partial z}+\lambda[b(z,\lambda)+c(z,\lambda)-(1+\gamma(z))^{-1}d(z,\lambda)]\frac{\partial\bar{h}}{\partial z}+\lambda d(z,\lambda)\frac{\partial\bar{s}}{\partial z}\right\}M_c(z)dz$$
$$+K_M(\lambda)M_B+F_C(\lambda)+F_M(\lambda), \quad \text{(B31)}$$

where

$$K_M(\lambda)\equiv[-\alpha(z_B)+\lambda a(z_B,\lambda)]\Delta s_v+\lambda[b(z_B,\lambda)+c(z_B,\lambda)]\Delta h+\lambda\frac{A(\lambda)}{\rho_B}, \quad \text{(B32)}$$

$$F_C(\lambda)\equiv\int_{z_B}^{z_D(\lambda)}\eta(z,\lambda)\left\{[-\alpha(z)+\lambda a(z,\lambda)]\left(\frac{\partial\bar{s}_v}{\partial t}\right)_{LS}\right.$$
$$\left.+\lambda[b(z,\lambda)+c(z,\lambda)-[1+\gamma(z)]^{-1}d(z,\lambda)]\left(\frac{\partial\bar{h}}{\partial t}\right)_{LS}+\lambda d(z,\lambda)\left(\frac{\partial\bar{s}}{\partial t}\right)_{LS}\right\}\rho(z)dz, \quad \text{(B33)}$$

$$F_M(\lambda)\equiv-K_M(\lambda)\rho_B\left(\frac{\partial z_B}{\partial t}\right)_{LS}+a(z_B,\lambda)\rho_B\frac{\partial s_{vM}}{\partial t}+[b(z_B,\lambda)+c(z_B,\lambda)]\rho_B\frac{\partial h_M}{\partial t}. \quad \text{(B34)}$$

We are restricting our attention to cases where $\Delta s_v>0$ and $\Delta q<0$. Under these conditions $z_C(\lambda_{\max})<z_D(\lambda_{\max})$ and $z_C(\lambda)\leqslant z_C(\lambda_{\max})$. Therefore $z_C(\lambda)<z_D(\lambda_{\max})$. This means that there is no detrainment between z_B and $z_C(\lambda)$, which allows us to drop $a(z,\lambda)\hat{l}(z)$ in the detrainment term of (B31). We can also change the lower limit of integration of the detrainment term to $z_D(\lambda_{\max})$ since there is no detrainment below this level. Substituting (77), (79) and (80) into (B31), and changing the detrainment term from an integral over z to an integral over λ', we obtain

$$\frac{\partial A(\lambda)}{\partial t}=\int_{\lambda}^{\lambda_{\max}}K_D(\lambda,\lambda')\mathfrak{M}_B(\lambda')d\lambda'+\int_{0}^{\lambda_{\max}}K_V(\lambda,\lambda')\mathfrak{M}_B(\lambda')d\lambda'+K_M(\lambda)M_B+F_C(\lambda)+F_M(\lambda), \quad \text{(B35)}$$

where

$$K_V(\lambda,\lambda')\equiv\int_{z_B}^{z_D(\lambda)}\eta(z,\lambda)\eta(z,\lambda')\left\{[-\alpha(z)+\lambda a(z,\lambda)]\frac{\partial\bar{s}_v}{\partial z}\right.$$
$$\left.+\lambda[b(z,\lambda)+c(z,\lambda)-[1+\gamma(z)]^{-1}d(z,\lambda)]\frac{\partial\bar{h}}{\partial z}+\lambda d(z,\lambda)\frac{\partial\bar{s}}{\partial z}\right\}dz, \quad \text{(B36)}$$

$$K_D(\lambda,\lambda')\equiv\eta(z_D',\lambda)\eta(z_D',\lambda')\{[1-(1+\delta)\epsilon(z_D')]\alpha(z_D')Ll(z_D')$$
$$+\lambda[b(z_D',\lambda)+c(z_D',\lambda)-(1+\gamma(z_D'))^{-1}d(z_D',\lambda)][\hat{h}^*(z_D')-\bar{h}^*(z_D')+L(\hat{q}^*(z_D')-\bar{q}(z_D'))]$$
$$+\lambda d(z_D',\lambda)[\hat{s}(z_D')-\bar{s}(z_D')-L\hat{l}(z_D')]\}, \quad \text{(B37)}$$

and where the symbol z_D' has been used for $z_D(\lambda')$. Defining

$$K_D(\lambda,\lambda')\equiv 0 \qquad \text{for} \qquad \lambda'<\lambda, \quad \text{(B38)}$$

and using (110), (143) and (144), (B35) can be written as (142).

Usually, the effect of liquid water in the buoyancy force is small. Then the terms which involve the coefficients $c(z,\lambda)$ and $d(z,\lambda)$ can be neglected.

REFERENCES

Arakawa, A., 1969: Parameterization of cumulus convection. *Proc. WMO/IUGG Symp. Numerical Weather Prediction*, Tokyo, 26 November–4 December, 1968, Japan Meteor. Agency, IV, 8, 1–6.

——, 1971: A parameterization of cumulus convection and its application to numerical simulation of the tropical general circulation. Paper presented at the 7th Tech. Conf. on Hurricanes and Tropical Meteorology, Barbados, Amer. Meteor. Soc.

——, 1972: Parameterization of cumulus convection. Design of the UCLA general circulation model. Numerical simulation of weather and climate, Tech. Rept. 7, Dept. of Meteorology, University of California, Los Angeles.

——, and W. Chao, 1973: A cumulus parameterization scheme and its applications. Paper presented at the 8th Tech. Conf. on Hurricanes and Tropical Meteorology, Key Biscayne, Amer. Meteor. Soc.

Árnason, G., R. S. Greenfield and E. A. Newburg, 1968: A numerical experiment in dry and moist convection including the rain state. *J. Atmos. Sci.*, **25**, 404–415.

——, P. S. Brown and R. T. Chu, 1969: Numerical simulation of the macrophysical and microphysical processes of moist convection. *Proc. WMO/IUGG Symp. Numerical Weather Prediction*, Tokyo, 26 November–4 December, 1968, Japan Meteor. Agency, I, 11–21.

——, and R. S. Greenfield, 1972: Micro- and macro-structures of numerically simulated convective clouds. *J. Atmos. Sci.*, **29**, 342–367.

Asai, T., and A. Kasahara, 1967: A theoretical study of the compensating downward motions associated with cumulus clouds. *J. Atmos. Sci.*, **24**, 487–496.

Ball, F. K., 1960: Control of inversion height by surface heating. *Quart. J. Roy. Meteor. Soc.*, **86**, 483–494.

Bates, J. R., 1972: Tropical disturbances and the general circulation. *Quart. J. Roy. Meteor. Soc.*, **98**, 1–16.

Betts, A. K., 1973a: Nonprecipitating cumulus convection and its parameterization. *Quart. J. Roy. Meteor. Soc.*, **99**, 178–196.

——, 1973b: A composite mesoscale cumulonimbus budget. *J. Atmos. Sci.*, **30**, 597–610.

Bjerknes, J., 1938: Saturated-adiabatic ascent of air through dry-

adiabatically descending environment. *Quart. J. Roy. Meteor. Soc.*, **64**, 325–330.

Bunker, A. F., B. Haurwitz, J. S. Malkus and H. Stommel, 1949: Vertical distribution of temperature and humidity over the Caribbean Sea. *Papers Phys. Oceanogr. Meteor.*, **11**, 82 pp.

Chao, W., S. Lord and A. Arakawa, 1974: A parameterization of cumulus convection for numerical models of the atmosphere. (To be published.)

Charney, J. G., and A. Eliassen, 1964: On the growth of the hurricane depression. *J. Atmos. Sci.*, **21**, 68–75.

Deardorff, J. W., 1972: Parameterization of the planetary boundary layer for use in general circulation models. *Mon. Wea. Rev.*, **100**, 93–106.

——, G. E. Willis and D. K. Lilly, 1969: Laboratory investigation of non-steady penetrative convection. *J. Fluid Mech.*, **35**, 7–31.

Gray, W. M., 1972: Cumulus convection and large-scale circulations, Part III. Broad scale and meso scale considerations. Atmos. Sci. Paper No. 190, Colorado State University, 80 pp.

Haltiner, G. J., 1971: *Numerical Weather Prediction*. New York, Wiley Inc., 317 pp.

Israeli, M., and E. S. Sarachik, 1973: Cumulus parameterization and CISK. *J. Atmos. Sci.*, **30**, 582–589.

Jordan, C. L., 1958: Mean soundings for the West Indies area. *J. Meteor.*, **15**, 91–97.

Kuo, H. L., 1965: On the formation and intensification of tropical cyclones through latent heat release by cumulus convection. *J. Atmos. Sci.*, **22**, 40–63.

Lilly, D. K., 1968: Models of cloud-topped mixed layers under a strong inversion. *Quart. J. Roy. Meteor. Soc.*, **94**, 292–309.

López, R. E., 1972a: Cumulus convection and larger scale circulations. Part I. A parametric model of cumulus convection. Atmos. Sci. Paper No. 188, Colorado State University, 100 pp.

——, 1972b: Cumulus convection and larger scale circulations. Part II. Cumulus and meso scale considerations. Atmos. Sci. Paper No. 189, Colorado State University, 63 pp.

Malkus, J. S., 1952: Recent advances in the study of convective clouds and their interaction with the environment. *Tellus*, **4**, 71–87.

——, 1958: On the structure of the trade wind moist layer. *Papers Phys. Oceanogr. Meteor.*, **13**, No. 2, 47 pp.

——, 1963: Cloud patterns over tropical oceans. *Science*, **141**, 767–778.

——, C. Ronne and M. Chaffee, 1961: Cloud patterns in hurricane Daisy, 1958. *Tellus*, **13**, 8–30.

Manabe, S., J. Smagorinsky and R. F. Strickler, 1965: Simulated climatology of a general circulation model with a hydrological cycle. *Mon. Wea. Rev.*, **93**, 769–798.

Murray, F. W., 1970: Numerical models of a tropical cumulus cloud with bilateral and axial symmetry. *Mon. Wea. Rev.*, **98**, 14–28.

——, and L. R. Koenig, 1972: Numerical experiments on the relation between microphysics and dynamics in cumulus convection. *Mon. Wea. Rev.*, **100**, 717–732.

Nitta, T., 1974: Observational determination of cloud mass flux distribution function. (Submitted to *J. Atmos. Sci.*).

Ogura, Y., 1972: Clouds and convection. Parameterization of Subgrid-Scale Processes, GARP Publ. Ser., No. 8, 20–39.

——, and N. A. Phillips, 1962: Scale analysis of deep and shallow convection in the atmosphere. *J. Atmos. Sci.* **19**, 173–179.

——, and T. Takahashi, 1971: Numerical simulation of the life cycle of a thunderstorm cell. *Mon. Wea. Rev.*, **99**, 895–911.

——, and H.-R. Cho, 1973: Diagnostic determination of cumulus cloud populations from observed large-scale variables. *J. Atmos. Sci.*, **30**, 1276–1286.

Ooyama, K., 1964: A dynamical model for the study of tropical cyclone development. *Geofis. Intern.*, **4**, 187–198.

——, 1969: Numerical simulation of the life cycle of tropical cyclones. *J. Atmos. Sci.*, **26**, 3–40.

——, 1971: A theory on parameterization of cumulus convection. *J. Meteor. Soc. Japan*, **49**, Special Issue, 744–756.

Orville, H. D., 1968: Ambient wind effects on the initiation of cumulus clouds over mountains. *J. Atmos. Sci.*, **25**, 385–403.

——, and L. J. Sloan, 1970: A numerical simulation of the life history of a rainstorm. *J. Atmos. Sci.*, **27**, 1148–1159.

Randall, D., and A. Arakawa, 1974: A parameterization of the planetary boundary layer for numerical models of the atmosphere. (To be published.)

Riehl, H., and J. S. Malkus, 1958: On the heat balance in the equatorial trough zone. *Geophysica*, **6**, 503–538.

——, and ——, 1961: Some aspects of hurricane Daisy, 1958. *Tellus*, **13**, 181–213.

Schubert, W. H., and A. Arakawa, 1974: Interaction of a cumulus cloud ensemble with the large-scale environment. Part II. (To be published.)

Simpson, J., 1971: On cumulus entrainment and one-dimensional models. *J. Atmos. Sci.*, **28**, 449–455.

——, R. H. Simpson, D. A. Andrews and M. A. Eaton, 1965: Experimental cumulus dynamics. *Rev. Geophys.*, **3**, 387–431.

——, and V. Wiggert, 1969: Models of precipitating cumulus towers. *Mon. Wea. Rev.*, **97**, 471–489.

——, and ——, 1971: 1968 Florida cumulus seeding experiment: Numerical model results. *Mon. Wea. Rev.*, **99**, 87–118.

Takeda, T., 1971: Numerical simulation of a precipitating convective cloud: The formation of a long-lasting cloud. *J. Atmos. Sci.*, **28**, 350–376.

Wilhelmson, R., and Y. Ogura, 1972: The pressure perturbation and the numerical modeling of a cloud. *J. Atmos. Sci.*, **29**, 1295–1307.

Yanai, M., 1961a: A detailed analysis of typhoon formation. *J. Meteor. Soc. Japan*, **39**, 187–214.

——, 1961b: Dynamical aspects of typhoon formation. *J. Meteor. Soc. Japan*, **39**, 283–309.

——, 1964: Formation of tropical cyclones. *Rev. Geophys.*, **2**, 367–414.

——, 1971a: A review of recent studies of tropical meteorology relevant to the planning of GATE. *Experimental Design Proposal by the Interim Scientific and Management Group (ISMG)*, Vol. 2, Annex 1.

——, 1971b: The mass, heat and moisture budgets and the convective heating within tropical cloud clusters. Paper presented at the 7th Tech. Conf. on Hurricanes and Tropical Meteorology, Barbados, Amer. Meteor. Soc.

——, S. Esbensen and J.-H. Chu, 1973: Determination of bulk properties of tropical cloud clusters from large scale heat and moisture budgets. *J. Atmos. Sci.*, **30**, 611–627.